Jian Wang, Yuping Su, Jianping Zheng, E.A. Belousova, Ming Chen, Hongkun Dai, and Liang Zhou, 2021, Rapid transition from oceanic subduction to postcollisional extension revealed by Carboniferous magmatism in East Junggar (NW China), southwestern Central Asian orogenic belt: GSA Bulletin, https://doi.org/10.1130/B36074.1.

# Supplemental Material

**Analytical methods**

**Figure S1.** Representative Cathodoluminescence images of zircon grains for the studied Carboniferous volcanic rocks. U-Pb dating pits are shown by small solid circles, and Lu-Hf analysis pits are shown by large, dotted circles.

**Figure S2.** Whole-rock $^{40}Ar$-$^{39}Ar$ dating for the BJE mafic dikes from the East Junggar.

**Table S1.** Zircon U-Pb data for the Carboniferous volcanic rocks from the East Junggar.

**Table S2.** Zircon trace element data for the Carboniferous volcanic rocks from the East Junggar.

**Table S3.** Whole-rock $^{40}Ar$-$^{39}Ar$ data for the BJE mafic dikes from the East Junggar.

**Table S4.** Whole-rock major and trace element data for the Carboniferous igneous rocks from the East Junggar.

**Table S5.** Zircon Hf isotope data for the Carboniferous volcanic rocks from the East Junggar.

**Table S6.** Whole-rock Sr-Nd isotope data for the Carboniferous igneous rocks from the East Junggar.

**Table S7.** Whole-rock Pb isotope data for the Carboniferous igneous rocks from the East Junggar.

**Table S8.** Trace element and isotope data for end-members used in geochemical modeling.

**Table S9.** Data source for non-modal batch melting.

**Table S10.** Key geological events in the East Junggar that place constraints on the closure time of the Kalamaili Ocean

## ANALYTICAL METHODS

### Zircon U-Pb Dating, Trace Element and Lu-Hf Isotopic Analyses

Zircons were separated by conventional heavy liquid and magnetic techniques at the Langfang Chengxin Geological Service Company (Hebei, China). Then they were handpicked under a binocular microscope, mounted in epoxy and polished to about half section. Cathodoluminescence (CL) images of zircon grains were taken on a Gatan Mono CL4 Cathode-Luminescence detector attached to a Zeiss Sigma 300 field emission SEM at the State Key Laboratory of Geological Processes and Mineral Resources, China University of Geosciences (CUG), Wuhan, to observe the internal structure and to target potential sites for zircon U-Pb-Hf isotopic analyses.

In situ zircon U-Pb dating and trace element compositions were simultaneously analyzed by LA-ICP-MS at the Wuhan SampleSolution Analytical Technology Co., Ltd., Hubei Province. Detailed operating conditions for the laser ablation system and the ICP-MS instrument and data reduction are the same as those described by Zong et al. (2017). Laser sampling was performed using a GeolasPro laser ablation system that consists of a COMPexPro 102 ArF excimer laser (wavelength of 193 nm and maximum energy of 200 mJ) and a MicroLas optical system. An Agilent 7700e ICP-MS instrument was applied to acquire ion-signal intensities. Helium was used as a carrier gas, and argon was employed as the make-up gas and mixed with the carrier gas via a T-connector before entering the ICP. In this study, the spot size and frequency of the laser were set to 32 μm and 5 Hz, respectively. For every five analyses, zircon 91500, GJ-1 and glass NIST610 were used as external standards for U-Pb dating and trace element calibration. Each analysis incorporated a background acquisition of ~20–30 s followed by 50 s of data acquisition from the sample. Raw data were processed using an Excel-based software ICPMSDataCal (Liu et al., 2010). Concordia diagrams and age calculations were made using the program Isoplot/Ex_ver3 (Ludwig, 2003).

In situ zircon Lu-Hf isotopic analysis was conducted using a Neptune Plus MC-ICP-MS (Thermo Fisher Scientific, Germany) in combination with a Geolas HD excimer ArF laser ablation system (Coherent, Göttingen, Germany) at the Wuhan Sample Solution Analytical Technology Co., Ltd, Hubei, China. A "wire" signal smoothing device is included in this laser ablation system (Hu et al., 2015), by which smooth signals are produced even at very low laser repetition rates down to 1 Hz. Helium was applied as the carrier gas within the ablation cell and was merged with argon (makeup gas) after the ablation cell. Small amounts of nitrogen were added to the argon makeup gas flow for the improvement of sensitivity of Hf isotopes (Hu et al. 2012). Compared to the standard arrangement, the addition of nitrogen in combination with the use of the newly designed X skimmer cone and Jet sample cone in Neptune Plus improved the signal intensity of Hf, Yb and Lu by a factor of 5.3, 4.0 and 2.4, respectively. In this study, all data were acquired on zircon in single spot ablation mode at a spot size of 44 μm, and the energy density of laser ablation was ~7.0 J $cm^{-2}$. Each measurement consisted of 20 s of acquisition of the background signal followed by 50 s of ablation signal acquisition. Detailed operating conditions for the laser ablation system and the MC-ICP-MS instrument and analytical method can be found in Hu et al. (2012). Off-line selection and integration of analyte signals, and mass bias calibrations were performed using ICPMSDataCal (Liu et al., 2010). The depleted mantle model ages ($T_{DM}$) and average crustal model ages ($T_{crust}$) were calculated by the methods suggested by Griffin et al. (2000).

## Whole-rock $^{40}Ar/^{39}Ar$ geochronology

As no zircon grains were separated from the BJE diabase dikes, two samples (BEJ-8 and BJE-9) were chosen for whole-rock $^{40}Ar/^{39}Ar$ dating based on rock freshness and relatively low calcium but high potassium contents. The rocks were first crushed into 40–60 mesh powders (250–425 μm), then removal of any visible impurities and phenocrysts, and final ultrasonically cleaned in distilled water and dried. The well-prepared samples and the monitor standard (ZBH-2506: 132.700 ± 0.027 Ma) were irradiated together for 54 h in the 49–2 nuclear reactor in Beijing. Step-heating $^{40}Ar/^{39}Ar$ analysis was performed using Noble Gas Mass Spectrometer Argus VI at the Key Laboratory of Tectonics and Petroleum Resources Ministry of Education, CUG, following analytical procedures described by Qiu et al. (2015). The ArArCALC software was used for data proceeding and plotting (Koppers, 2002).

## Whole-rock Major and Trace Element Analyses

Whole-rock major and trace element compositions were measured at the State Key Laboratory of Geological Processes and Mineral Resources, CUG. Major oxides were analyzed by X-ray fluorescence (XRF) using a Shimadzu XRF-1800 sequential XRF system, following methods described by Ma et al. (2012). Chinese national rock standards (GBW07105, basalt; GBW07104, andesite; GBW07113, rhyolite) were used to monitor the data quality. Analytical precision for major oxides is commonly better than 5%. Trace elements were measured on an Agilent 7500a ICP-MS instrument, and the analytical conditions and procedures can be found in Liu et al. (2008). National rock standards (AGV-2, BHVO-2, RCR-2 and RGM-2) were selected for calibrating element concentrations of the analyzed samples. Analytical uncertainties for most trace elements are generally less than 5%.

## Whole-rock Sr-Nd-Pb isotopic analyses

Whole-rock Sr-Nd-Pb isotopic analyses were carried out on a Neptune Plus MC-ICP-MS (Thermo Fisher Scientific, Dreieich, Germany) at the Wuhan Sample Solution Analytical Technology Co., Ltd, Hubei, China. All chemical preparations were made on class 100 work benches within a class 1000 over-pressured clean laboratory. The detailed methods and instrumentation for Sr-Nd and Pb isotopic analyses have been described by Li et al. (2012) and Baker et al. (2004), respectively. During the Sr-Nd isotopic analyses, the NIST SRM 987 standard solution yielded $^{87}Sr/^{86}Sr$ ratio of 0.710244 ± 0.000022 (2SD, n = 32) and the JNdi-1 standard gave $^{143}Nd/^{144}Nd$ ratio of 0.512118 ± 0.000015 (2SD, n = 31). In addition, the USGS reference materials BCR-2 (basalt) and RGM-2 (rhyolite) yielded results of 0.705034 ± 0.000014 (2SD, n = 4) and 0.704192 ± 0.000010 (2SD, n = 4) for $^{87}Sr/^{86}Sr$, 0.512644 ± 0.000015 (2SD, n = 6) and 0.512810 ± 0.000015 (2SD, n = 4) for $^{143}Nd/^{144}Nd$, respectively, both of which are identical within error to their published values (Li et al., 2012). All measured $^{20x}Pb/^{204}Pb$ ratios of unknown samples were normalized to the well-accepted NBS SRM 981 values of $^{208}Pb/^{204}Pb$ = 36.7262 ± 0.0031, $^{207}Pb/^{204}Pb$ = 15.5000 ± 0.0013, $^{206}Pb/^{204}Pb$ = 16.9416 ± 0.0013 (Baker et al., 2004). Analyses of NBS SRM 981 standard yielded external precisions of 0.03% (2RSD) for $^{20x}Pb/^{204}Pb$ ratios. In addition, the USGS reference materials BCR-2 (basalt) gave results of $^{208}Pb/^{204}Pb$ = 38.743 ± 0.017, $^{207}Pb/^{204}Pb$ = 15.624 ± 0.003, $^{206}Pb/^{204}Pb$ = 18.763 ± 0.008 (2SD, n = 4), respectively, which are identical within error of 0.03% to their published values (Baker et al., 2004).

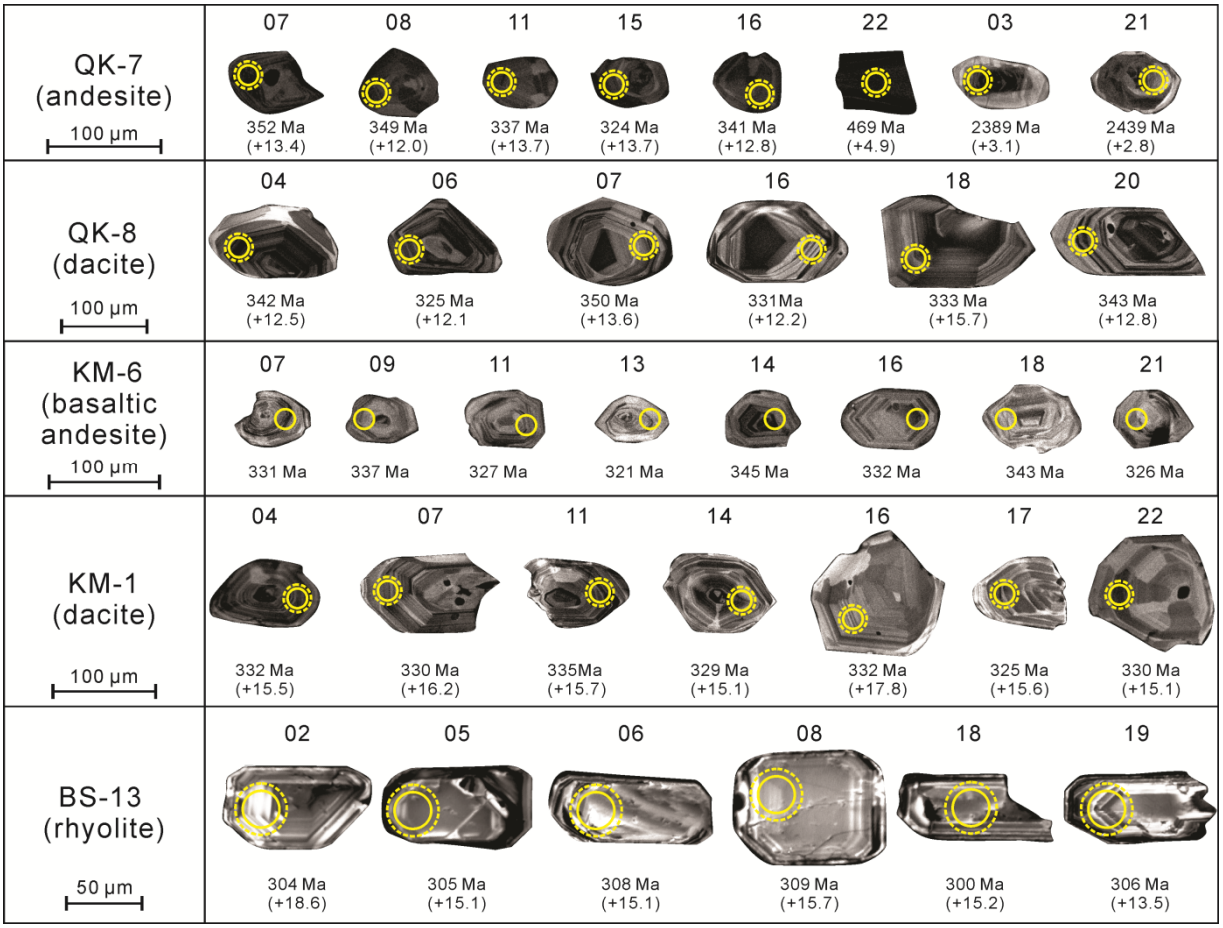


**Figure S1.** Representative Cathodoluminescence images of zircon grains for the studied Carboniferous volcanic rocks. U-Pb dating pits are shown by small solid circles, and Lu-Hf analysis pits are shown by large dotted circles.

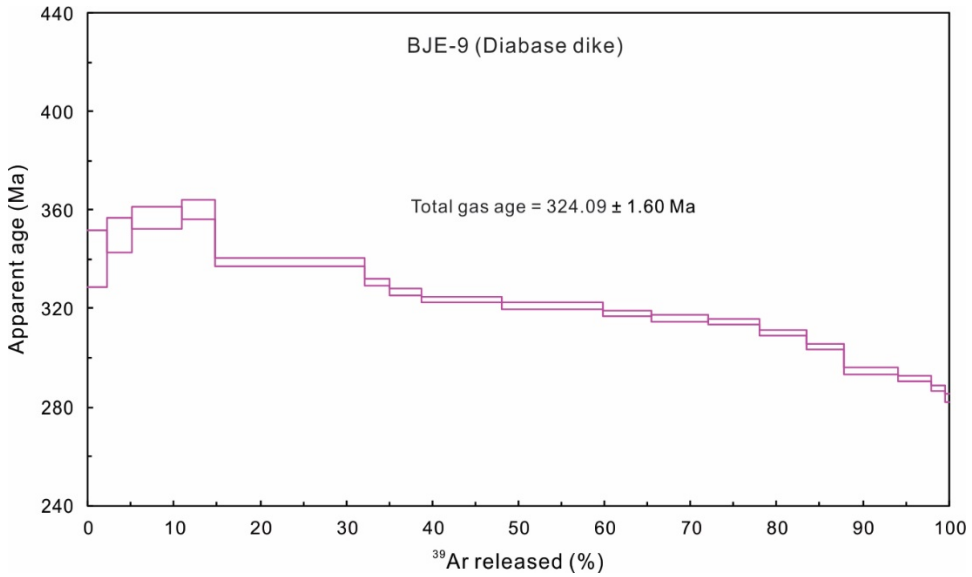


124

125 **Figure S2.** Whole-rock $^{40}Ar$-$^{39}Ar$ dating for the BJE mafic dikes from the East Junggar.

**Table S1.** Zircon U-Pb data for the studied Carboniferous volcanic rocks from the East Junggar.

| Analysis spot | Th (ppm) | U (ppm) | Th/U | Atomic ratios | | | | | | Ages (Ma) | | | | | | Concordance (%) |
|---|---|---|---|---|---|---|---|---|---|---|---|---|---|---|---|---|
| | | | | $^{207}Pb/^{206}Pb$ | 1σ | $^{207}Pb/^{235}U$ | 1σ | $^{206}Pb/^{238}U$ | 1σ | $^{207}Pb/^{206}Pb$ | 1σ | $^{207}Pb/^{235}U$ | 1σ | $^{206}Pb/^{238}U$ | 1σ | |
| Sample: QK-7 (Andesite) | | | | | | | | | | | | | | | | |
| QK-7-02 | 43.8 | 84.3 | 0.52 | 0.0571 | 0.0032 | 0.4317 | 0.0314 | 0.0560 | 0.0015 | 494 | 122 | 364 | 22 | 351 | 9 | 96% |
| QK-7-03 | 113 | 193 | 0.59 | 0.1529 | 0.0021 | 9.4010 | 0.7152 | 0.4420 | 0.0088 | 2389 | 23 | 2378 | 70 | 2360 | 39 | 99% |
| QK-7-04 | 42.5 | 92.8 | 0.46 | 0.0662 | 0.0030 | 0.5343 | 0.0566 | 0.0593 | 0.0012 | 813 | 94 | 435 | 37 | 371 | 7 | 84% |
| QK-7-05 | 212 | 385 | 0.55 | 0.1532 | 0.0014 | 9.1840 | 1.1020 | 0.4318 | 0.0068 | 2383 | 16 | 2357 | 110 | 2314 | 31 | 98% |
| QK-7-07 | 42.9 | 74.5 | 0.58 | 0.0582 | 0.0038 | 0.4383 | 0.0790 | 0.0561 | 0.0016 | 539 | 141 | 369 | 56 | 352 | 10 | 95% |
| QK-7-08 | 55.5 | 99.4 | 0.56 | 0.0624 | 0.0036 | 0.4774 | 0.0816 | 0.0556 | 0.0013 | 687 | 122 | 396 | 56 | 349 | 8 | 87% |
| QK-7-09 | 271 | 393 | 0.69 | 0.0660 | 0.0013 | 0.6964 | 0.1176 | 0.0767 | 0.0010 | 809 | 43 | 537 | 70 | 476 | 6 | 88% |
| QK-7-10 | 171 | 287 | 0.60 | 0.1526 | 0.0009 | 10.548 | 1.9990 | 0.4992 | 0.0050 | 2376 | 11 | 2484 | 178 | 2610 | 22 | 95% |
| QK-7-11 | 38.3 | 84.0 | 0.46 | 0.0550 | 0.0030 | 0.4003 | 0.0930 | 0.0536 | 0.0013 | 409 | 124 | 342 | 68 | 337 | 8 | 98% |
| QK-7-12 | 333 | 615 | 0.54 | 0.1503 | 0.0007 | 8.4728 | 2.2853 | 0.4078 | 0.0053 | 2350 | 8 | 2283 | 250 | 2205 | 24 | 96% |
| QK-7-14 | 48.1 | 88.2 | 0.54 | 0.0619 | 0.0031 | 0.4576 | 0.0978 | 0.0542 | 0.0014 | 733 | 104 | 383 | 68 | 340 | 9 | 88% |
| QK-7-15 | 42.4 | 99.2 | 0.43 | 0.0587 | 0.0038 | 0.4087 | 0.0742 | 0.0515 | 0.0014 | 567 | 145 | 348 | 54 | 324 | 8 | 92% |
| QK-7-16 | 555 | 360 | 1.54 | 0.0924 | 0.0028 | 0.6938 | 0.0914 | 0.0543 | 0.0010 | 1476 | 57 | 535 | 55 | 341 | 6 | 55% |
| QK-7-17 | 37.9 | 76.0 | 0.50 | 0.0660 | 0.0038 | 0.4661 | 0.0486 | 0.0516 | 0.0015 | 806 | 120 | 388 | 34 | 325 | 9 | 82% |
| QK-7-18 | 151 | 232 | 0.65 | 0.1567 | 0.0028 | 8.9734 | 0.4515 | 0.4142 | 0.0089 | 2421 | 30 | 2335 | 46 | 2234 | 40 | 95% |
| QK-7-21 | 282 | 378 | 0.74 | 0.1583 | 0.0020 | 10.250 | 1.7263 | 0.4661 | 0.0065 | 2439 | 23 | 2458 | 157 | 2467 | 29 | 99% |
| QK-7-22 | 361 | 252 | 1.43 | 0.0924 | 0.0020 | 0.9692 | 0.2198 | 0.0755 | 0.0012 | 1476 | 41 | 688 | 114 | 469 | 7 | 62% |
| QK-7-23 | 173 | 280 | 0.62 | 0.1536 | 0.0018 | 9.9156 | 2.8256 | 0.4673 | 0.0087 | 2387 | 20 | 2427 | 269 | 2472 | 38 | 98% |
| Sample: QK-8 (Dacite) | | | | | | | | | | | | | | | | |
| QK-8-01 | 47.9 | 80.5 | 0.60 | 0.0551 | 0.0033 | 0.3946 | 0.0230 | 0.0527 | 0.0010 | 417 | 133 | 338 | 17 | 331 | 6 | 98% |
| QK-8-02 | 122 | 172 | 0.71 | 0.0538 | 0.0023 | 0.4186 | 0.0165 | 0.0570 | 0.0008 | 361 | 94 | 355 | 12 | 357 | 5 | 99% |
| QK-8-03 | 29.2 | 49.1 | 0.59 | 0.0662 | 0.0051 | 0.4986 | 0.0379 | 0.0564 | 0.0016 | 813 | 162 | 411 | 26 | 354 | 10 | 85% |
| QK-8-04 | 194 | 212 | 0.91 | 0.0538 | 0.0022 | 0.4036 | 0.0159 | 0.0545 | 0.0007 | 361 | 58 | 344 | 12 | 342 | 4 | 99% |
| QK-8-05 | 102 | 131 | 0.78 | 0.0553 | 0.0033 | 0.4073 | 0.0232 | 0.0542 | 0.0010 | 433 | 131 | 347 | 17 | 340 | 6 | 98% |
| QK-8-06 | 57.2 | 98.1 | 0.58 | 0.0577 | 0.0033 | 0.4043 | 0.0222 | 0.0517 | 0.0009 | 520 | 126 | 345 | 16 | 325 | 6 | 94% |
| QK-8-07 | 40.9 | 53.7 | 0.76 | 0.0743 | 0.0059 | 0.5500 | 0.0431 | 0.0558 | 0.0015 | 1051 | 160 | 445 | 28 | 350 | 9 | 76% |
| QK-8-08 | 77.1 | 96.6 | 0.80 | 0.0529 | 0.0029 | 0.3992 | 0.0216 | 0.0550 | 0.0009 | 324 | 124 | 341 | 16 | 345 | 6 | 98% |
| QK-8-09 | 58.3 | 86.0 | 0.68 | 0.0564 | 0.0037 | 0.4110 | 0.0273 | 0.0532 | 0.0012 | 478 | 144 | 350 | 20 | 334 | 7 | 95% |

| | | | | | | | | | | | | | | | | |
|---|---|---|---|---|---|---|---|---|---|---|---|---|---|---|---|---|
| QK-8-10 | 79.7 | 91.9 | 0.87 | 0.0551 | 0.0031 | 0.4094 | 0.0215 | 0.0553 | 0.0009 | 417 | 156 | 348 | 15 | 347 | 6 | 99% |
| QK-8-11 | 330 | 304 | 1.09 | 0.0532 | 0.0017 | 0.4040 | 0.0129 | 0.0547 | 0.0006 | 339 | 72 | 345 | 9 | 343 | 4 | 99% |
| QK-8-12 | 67.3 | 97.5 | 0.69 | 0.0727 | 0.0042 | 0.5317 | 0.0285 | 0.0536 | 0.0010 | 1006 | 119 | 433 | 19 | 337 | 6 | 74% |
| QK-8-13 | 63.9 | 91.5 | 0.70 | 0.0545 | 0.0030 | 0.4222 | 0.0223 | 0.0565 | 0.0009 | 391 | 129 | 358 | 16 | 354 | 5 | 99% |
| QK-8-14 | 95.8 | 117 | 0.82 | 0.0614 | 0.0033 | 0.4378 | 0.0216 | 0.0523 | 0.0008 | 654 | 82 | 369 | 15 | 329 | 5 | 88% |
| QK-8-15 | 656 | 436 | 1.50 | 0.0561 | 0.0022 | 0.4351 | 0.0173 | 0.0558 | 0.0007 | 457 | 89 | 367 | 12 | 350 | 4 | 95% |
| QK-8-16 | 59.1 | 84.7 | 0.70 | 0.0555 | 0.0032 | 0.3950 | 0.0220 | 0.0527 | 0.0009 | 432 | 134 | 338 | 16 | 331 | 6 | 97% |
| QK-8-17 | 48.9 | 59.8 | 0.82 | 0.0635 | 0.0052 | 0.4530 | 0.0329 | 0.0540 | 0.0015 | 728 | 179 | 379 | 23 | 339 | 9 | 88% |
| QK-8-18 | 87.6 | 125 | 0.70 | 0.0529 | 0.0027 | 0.3862 | 0.0193 | 0.0530 | 0.0008 | 324 | 114 | 332 | 14 | 333 | 5 | 99% |
| QK-8-19 | 83.4 | 114 | 0.73 | 0.0566 | 0.0037 | 0.4354 | 0.0254 | 0.0574 | 0.0013 | 476 | 144 | 367 | 18 | 360 | 8 | 97% |
| QK-8-20 | 44.6 | 70.1 | 0.64 | 0.0564 | 0.0044 | 0.4067 | 0.0283 | 0.0547 | 0.0012 | 478 | 172 | 346 | 20 | 343 | 7 | 99% |
| QK-8-21 | 599 | 494 | 1.21 | 0.0531 | 0.0013 | 0.3988 | 0.0097 | 0.0542 | 0.0005 | 345 | 56 | 341 | 7 | 340 | 3 | 99% |
| QK-8-22 | 53.4 | 85.8 | 0.62 | 0.0603 | 0.0045 | 0.4070 | 0.0273 | 0.0506 | 0.0009 | 613 | 163 | 347 | 20 | 318 | 5 | 91% |
| Sample: KM-6 (Basaltic andesite) | | | | | | | | | | | | | | | | |
| KM-6-07 | 297 | 284 | 1.05 | 0.0533 | 0.0019 | 0.3859 | 0.0136 | 0.0526 | 0.0006 | 339 | 81 | 331 | 10 | 331 | 4 | 99% |
| KM-6-08 | 167 | 187 | 0.90 | 0.0534 | 0.0027 | 0.3953 | 0.0203 | 0.0537 | 0.0008 | 346 | 112 | 338 | 15 | 337 | 5 | 99% |
| KM-6-09 | 85.1 | 112 | 0.76 | 0.0538 | 0.0026 | 0.3952 | 0.0190 | 0.0537 | 0.0008 | 365 | 114 | 338 | 14 | 337 | 5 | 99% |
| KM-6-11 | 91.3 | 116 | 0.78 | 0.0544 | 0.0025 | 0.3864 | 0.0171 | 0.0521 | 0.0008 | 387 | 102 | 332 | 13 | 327 | 5 | 98% |
| KM-6-12 | 125 | 157 | 0.80 | 0.0544 | 0.0024 | 0.4005 | 0.0166 | 0.0545 | 0.0008 | 387 | 98 | 342 | 12 | 342 | 5 | 99% |
| KM-6-13 | 176 | 230 | 0.77 | 0.0533 | 0.0020 | 0.3729 | 0.0132 | 0.0511 | 0.0006 | 343 | 88 | 322 | 10 | 321 | 4 | 99% |
| KM-6-14 | 95.0 | 123 | 0.77 | 0.0550 | 0.0030 | 0.4041 | 0.0208 | 0.0549 | 0.0008 | 413 | 122 | 345 | 15 | 345 | 5 | 99% |
| KM-6-15 | 74.4 | 96.1 | 0.77 | 0.0542 | 0.0029 | 0.4025 | 0.0209 | 0.0545 | 0.0008 | 389 | 122 | 343 | 15 | 342 | 5 | 99% |
| KM-6-16 | 115 | 134 | 0.86 | 0.0541 | 0.0024 | 0.3871 | 0.0166 | 0.0528 | 0.0007 | 376 | 100 | 332 | 12 | 332 | 4 | 99% |
| KM-6-17 | 112 | 153 | 0.73 | 0.0536 | 0.0021 | 0.3920 | 0.0142 | 0.0535 | 0.0006 | 354 | 87 | 336 | 10 | 336 | 4 | 99% |
| KM-6-18 | 89.1 | 111 | 0.80 | 0.0539 | 0.0030 | 0.4033 | 0.0227 | 0.0547 | 0.0008 | 365 | 124 | 344 | 16 | 343 | 5 | 99% |
| KM-6-19 | 79.6 | 104 | 0.77 | 0.0539 | 0.0033 | 0.3795 | 0.0223 | 0.0517 | 0.0008 | 365 | 141 | 327 | 16 | 325 | 5 | 99% |
| KM-6-20 | 135 | 176 | 0.76 | 0.0569 | 0.0032 | 0.4172 | 0.0229 | 0.0533 | 0.0008 | 487 | 121 | 354 | 16 | 335 | 5 | 94% |
| KM-6-21 | 91.1 | 163 | 0.56 | 0.0541 | 0.0026 | 0.3845 | 0.0176 | 0.0518 | 0.0008 | 376 | 107 | 330 | 13 | 326 | 5 | 98% |
| Sample: KM-1 (Dacite) | | | | | | | | | | | | | | | | |
| KM-1-01 | 491 | 470 | 1.05 | 0.0533 | 0.0015 | 0.3741 | 0.0108 | 0.0507 | 0.0005 | 343 | 65 | 323 | 8 | 319 | 3 | 98% |
| KM-1-02 | 603 | 479 | 1.26 | 0.0540 | 0.0013 | 0.3860 | 0.0097 | 0.0516 | 0.0005 | 369 | 56 | 331 | 7 | 324 | 3 | 97% |
| KM-1-04 | 167 | 162 | 1.03 | 0.0586 | 0.0023 | 0.4231 | 0.0156 | 0.0529 | 0.0007 | 554 | 87 | 358 | 11 | 332 | 4 | 92% |

| | | | | | | | | | | | | | | | |
|---|---|---|---|---|---|---|---|---|---|---|---|---|---|---|---|
| KM-1-05 | 40.4 | 58.2 | 0.69 | 0.0610 | 0.0045 | 0.4173 | 0.0270 | 0.0528 | 0.0012 | 639 | 159 | 354 | 19 | 332 | 8 | 93% |
| KM-1-07 | 189 | 130 | 1.45 | 0.0535 | 0.0024 | 0.3848 | 0.0161 | 0.0526 | 0.0007 | 350 | 100 | 331 | 12 | 330 | 4 | 99% |
| KM-1-08 | 797 | 634 | 1.26 | 0.0537 | 0.0013 | 0.4007 | 0.0096 | 0.0539 | 0.0005 | 361 | 56 | 342 | 7 | 338 | 3 | 98% |
| KM-1-10 | 407 | 440 | 0.93 | 0.0523 | 0.0014 | 0.3699 | 0.0095 | 0.0513 | 0.0006 | 298 | 66 | 320 | 7 | 322 | 3 | 99% |
| KM-1-11 | 345 | 430 | 0.80 | 0.0533 | 0.0013 | 0.3945 | 0.0095 | 0.0533 | 0.0006 | 343 | 56 | 338 | 7 | 335 | 3 | 99% |
| KM-1-14 | 32.1 | 76.4 | 0.42 | 0.0535 | 0.0028 | 0.3808 | 0.0192 | 0.0523 | 0.0009 | 350 | 116 | 328 | 14 | 329 | 6 | 99% |
| KM-1-15 | 440 | 464 | 0.95 | 0.0540 | 0.0014 | 0.4026 | 0.0102 | 0.0538 | 0.0006 | 372 | 59 | 344 | 7 | 338 | 4 | 98% |
| KM-1-16 | 97.6 | 130 | 0.75 | 0.0548 | 0.0027 | 0.3908 | 0.0176 | 0.0529 | 0.0008 | 406 | 118 | 335 | 13 | 332 | 5 | 99% |
| KM-1-17 | 113 | 121 | 0.94 | 0.0537 | 0.0026 | 0.3823 | 0.0173 | 0.0517 | 0.0008 | 367 | 109 | 329 | 13 | 325 | 5 | 98% |
| KM-1-18 | 849 | 375 | 2.26 | 0.0526 | 0.0013 | 0.3811 | 0.0099 | 0.0520 | 0.0005 | 322 | 57 | 328 | 7 | 327 | 3 | 99% |
| KM-1-19 | 94.2 | 128 | 0.74 | 0.0524 | 0.0022 | 0.3707 | 0.0164 | 0.0509 | 0.0007 | 306 | 96 | 320 | 12 | 320 | 4 | 99% |
| KM-1-22 | 129 | 144 | 0.90 | 0.0536 | 0.0023 | 0.3859 | 0.0165 | 0.0526 | 0.0007 | 367 | 100 | 331 | 12 | 330 | 5 | 99% |
| Sample: BS-13 (Rhyolite) | | | | | | | | | | | | | | | | |
| BS-13-01 | 180 | 273 | 0.66 | 0.0550 | 0.0023 | 0.3610 | 0.0145 | 0.0477 | 0.0006 | 409 | 93 | 313 | 11 | 300 | 4 | 95% |
| BS-13-02 | 392 | 501 | 0.78 | 0.0599 | 0.0016 | 0.3984 | 0.0099 | 0.0482 | 0.0004 | 598 | 59 | 340 | 7 | 304 | 2 | 88% |
| BS-13-03 | 167 | 213 | 0.78 | 0.0535 | 0.0023 | 0.3625 | 0.0148 | 0.0495 | 0.0007 | 350 | 96 | 314 | 11 | 312 | 4 | 99% |
| BS-13-04 | 782 | 1007 | 0.78 | 0.0667 | 0.0022 | 0.4496 | 0.0177 | 0.0483 | 0.0008 | 829 | 67 | 377 | 12 | 304 | 5 | 78% |
| BS-13-05 | 229 | 343 | 0.67 | 0.0531 | 0.0022 | 0.3530 | 0.0135 | 0.0484 | 0.0006 | 345 | 97 | 307 | 10 | 305 | 4 | 99% |
| BS-13-06 | 208 | 262 | 0.79 | 0.0518 | 0.0030 | 0.3512 | 0.0201 | 0.0490 | 0.0006 | 280 | 131 | 306 | 15 | 308 | 4 | 99% |
| BS-13-08 | 304 | 297 | 1.02 | 0.0580 | 0.0055 | 0.3954 | 0.0387 | 0.0491 | 0.0009 | 528 | 209 | 338 | 28 | 309 | 6 | 90% |
| BS-13-10 | 421 | 702 | 0.60 | 0.0516 | 0.0016 | 0.3533 | 0.0113 | 0.0492 | 0.0006 | 333 | 72 | 307 | 9 | 310 | 4 | 99% |
| BS-13-12 | 69.9 | 152 | 0.46 | 0.0532 | 0.0023 | 0.3519 | 0.0149 | 0.0480 | 0.0006 | 345 | 98 | 306 | 11 | 302 | 3 | 98% |
| BS-13-18 | 520 | 598 | 0.87 | 0.0539 | 0.0017 | 0.3557 | 0.0116 | 0.0477 | 0.0006 | 365 | 68 | 309 | 9 | 300 | 3 | 97% |
| BS-13-19 | 122 | 198 | 0.61 | 0.0520 | 0.0036 | 0.3510 | 0.0263 | 0.0487 | 0.0010 | 283 | 156 | 306 | 20 | 306 | 6 | 99% |
| BS-13-22 | 190 | 282 | 0.68 | 0.0521 | 0.0031 | 0.3484 | 0.0213 | 0.0487 | 0.0007 | 300 | 137 | 304 | 16 | 306 | 4 | 99% |
| BS-13-23 | 72.3 | 158 | 0.46 | 0.0524 | 0.0046 | 0.3548 | 0.0317 | 0.0490 | 0.0009 | 302 | 206 | 308 | 24 | 309 | 6 | 99% |
| BS-13-24 | 435 | 607 | 0.72 | 0.0532 | 0.0022 | 0.3598 | 0.0142 | 0.0488 | 0.0005 | 345 | 95 | 312 | 11 | 307 | 3 | 98% |
| BS-13-25 | 233 | 311 | 0.75 | 0.0590 | 0.0030 | 0.3962 | 0.0190 | 0.0487 | 0.0009 | 569 | 109 | 339 | 14 | 306 | 5 | 89% |
| BS-13-26 | 344 | 414 | 0.83 | 0.0534 | 0.0025 | 0.3457 | 0.0159 | 0.0469 | 0.0006 | 346 | 106 | 301 | 12 | 296 | 4 | 98% |
| BS-13-27 | 149 | 236 | 0.63 | 0.0508 | 0.0021 | 0.3405 | 0.0131 | 0.0487 | 0.0005 | 232 | 62 | 298 | 10 | 307 | 3 | 96% |
| BS-13-28 | 449 | 766 | 0.59 | 0.0543 | 0.0016 | 0.3644 | 0.0109 | 0.0483 | 0.0005 | 383 | 69 | 316 | 8 | 304 | 3 | 96% |
| BS-13-30 | 427 | 581 | 0.74 | 0.0536 | 0.0017 | 0.3588 | 0.0111 | 0.0484 | 0.0007 | 354 | 77 | 311 | 8 | 304 | 4 | 97% |

**Table S2.** Zircon trace element data for the studied Carboniferous volcanic rocks from the East Junggar.

| Analytical No. | $T_{Zr}$ (°C) | $fO_2$ (ΔFMQ) | Trace elements (ppm) | | | | | | | | | | | | | | | | | | |
|---|---|---|---|---|---|---|---|---|---|---|---|---|---|---|---|---|---|---|---|---|---|
| | | | Ti | U | Y | Nb | La | Ce | Pr | Nd | Sm | Eu | Gd | Tb | Dy | Ho | Er | Tm | Yb | Lu | Hf | Ta |
| Sample: QK-7 (Andesite) | | | | | | | | | | | | | | | | | | | | | | |
| QK-7-02 | 750 | -0.61 | 11.0 | 84.3 | 1068 | 1.73 | 0.02 | 5.77 | 0.20 | 3.24 | 5.42 | 1.39 | 26.5 | 8.55 | 102 | 33.4 | 149 | 31.6 | 311 | 49.2 | 7875 | 0.69 |
| QK-7-03 | 769 | 0.29 | 13.6 | 193 | 650 | 1.70 | 0.14 | 16.3 | 0.13 | 1.76 | 3.64 | 0.57 | 15.3 | 4.41 | 52.6 | 19.0 | 92.1 | 19.9 | 208 | 36.0 | 10198 | 0.94 |
| QK-7-04 | 737 | -0.36 | 9.53 | 92.8 | 716 | 1.96 | 0.01 | 6.49 | 0.072 | 1.36 | 2.80 | 0.79 | 16.5 | 5.14 | 62.8 | 21.9 | 102 | 21.8 | 227 | 36.5 | 7951 | 0.90 |
| QK-7-05 | 821 | 1.16 | 23.3 | 385 | 706 | 2.35 | 12.8 | 49.4 | 2.83 | 11.6 | 3.94 | 0.94 | 14.0 | 4.30 | 53.4 | 19.6 | 97.7 | 22.6 | 257 | 44.0 | 10791 | 1.51 |
| QK-7-07 | 938 | -1.85 | 65.2 | 74.5 | 942 | 1.38 | 0.02 | 6.46 | 0.12 | 2.63 | 6.22 | 1.58 | 27.6 | 7.73 | 92.9 | 30.2 | 135 | 26.8 | 271 | 43.1 | 7937 | 0.52 |
| QK-7-08 | 867 | -0.63 | 35.9 | 99.4 | 1173 | 2.05 | 1.72 | 11.2 | 0.73 | 6.19 | 6.68 | 1.77 | 30.8 | 9.15 | 111 | 37.0 | 167 | 34.3 | 341 | 54.9 | 7674 | 0.92 |
| QK-7-09 | 792 | -0.84 | 17.3 | 393 | 1185 | 2.95 | 0.03 | 13.7 | 0.11 | 1.93 | 3.93 | 0.98 | 20.2 | 7.10 | 87.2 | 34.7 | 173 | 40.7 | 432 | 77.5 | 10678 | 1.65 |
| QK-7-10 | 754 | 0.06 | 11.6 | 287 | 1527 | 3.43 | 0.02 | 16.0 | 0.23 | 5.19 | 9.14 | 0.33 | 42.6 | 12.5 | 145 | 48.1 | 207 | 42.0 | 408 | 64.8 | 9575 | 1.11 |
| QK-7-11 | 753 | -0.51 | 11.5 | 84.0 | 814 | 1.78 | 0.03 | 6.22 | 0.10 | 1.90 | 4.10 | 1.09 | 19.0 | 5.99 | 74.9 | 25.8 | 117 | 24.4 | 253 | 42.7 | 7993 | 0.78 |
| QK-7-12 | 1022 | 1.47 | 122 | 615 | 1476 | 4.43 | 76.6 | 172 | 19.3 | 90.8 | 21.7 | 1.94 | 42.8 | 11.1 | 128 | 44.9 | 206 | 43.9 | 446 | 72.3 | 12088 | 1.87 |
| QK-7-14 | 805 | -0.94 | 19.9 | 88.2 | 1165 | 2.18 | 0.04 | 6.54 | 0.23 | 3.87 | 6.64 | 1.76 | 30.0 | 8.85 | 110 | 37.3 | 166 | 34.4 | 341 | 55.0 | 8093 | 0.80 |
| QK-7-15 | 780 | -1.00 | 15.4 | 99.2 | 846 | 2.35 | 0.01 | 5.89 | 0.09 | 1.75 | 3.28 | 0.97 | 18.5 | 6.23 | 73.7 | 27.0 | 123 | 25.5 | 260 | 44.5 | 8175 | 0.96 |
| QK-7-16 | 808 | 1.29 | 20.4 | 360 | 2131 | 12.6 | 0.17 | 48.2 | 0.20 | 3.63 | 7.95 | 3.01 | 43.4 | 15.2 | 182 | 63.8 | 290 | 60.3 | 592 | 100 | 7824 | 3.86 |
| QK-7-17 | 754 | -0.17 | 11.6 | 76.0 | 775 | 2.12 | 0.23 | 7.23 | 0.13 | 1.47 | 3.53 | 0.88 | 16.7 | 5.89 | 70.0 | 24.6 | 114 | 24.9 | 251 | 43.8 | 8087 | 1.09 |
| QK-7-18 | 916 | 0.96 | 54.7 | 232 | 508 | 2.11 | 19.5 | 52.6 | 3.76 | 16.1 | 3.77 | 0.83 | 11.7 | 3.46 | 39.9 | 14.3 | 71.8 | 17.5 | 192 | 35.8 | 11660 | 0.97 |
| QK-7-21 | 764 | 0.94 | 12.9 | 378 | 1492 | 4.73 | 0.12 | 32.2 | 0.20 | 4.03 | 7.93 | 0.49 | 37.8 | 11.2 | 134 | 47.4 | 208 | 42.5 | 422 | 69.6 | 10687 | 1.46 |
| QK-7-22 | 800 | 0.01 | 18.8 | 252 | 2144 | 1.92 | 0.45 | 18.6 | 0.64 | 8.34 | 12.4 | 2.82 | 57.1 | 17.0 | 199 | 65.8 | 282 | 55.7 | 535 | 87.3 | 9276 | 1.09 |
| QK-7-23 | 831 | 1.11 | 25.7 | 280 | 1321 | 3.34 | 3.34 | 43.0 | 62.9 | 209 | 24.4 | 3.90 | 41.5 | 10.6 | 119 | 41.1 | 186 | 39.3 | 394 | 65.7 | 9632 | 1.09 |
| Sample: QK-8 (Dacite) | | | | | | | | | | | | | | | | | | | | | | |
| QK-8-01 | 771 | -0.60 | 14.0 | 80.5 | 803 | 0.71 | 0.01 | 6.37 | 0.05 | 1.06 | 2.34 | 0.49 | 14.8 | 4.86 | 68.3 | 24.4 | 120 | 25.9 | 271 | 44.8 | 8769 | 0.38 |
| QK-8-02 | 767 | -0.37 | 13.4 | 172 | 1212 | 1.06 | 1.28 | 10.4 | 0.53 | 3.45 | 3.85 | 0.85 | 20.7 | 7.16 | 100 | 37.2 | 181 | 39.5 | 416 | 68.6 | 7909 | 0.52 |
| QK-8-03 | 821 | -0.80 | 23.3 | 49.1 | 552 | 0.59 | 0.097 | 5.72 | 0.05 | 0.93 | 1.39 | 0.26 | 8.73 | 3.27 | 45.0 | 16.4 | 82.4 | 18.5 | 195 | 32.1 | 8815 | 0.29 |
| QK-8-04 | 778 | 0.15 | 15.1 | 212 | 1497 | 1.43 | 1.17 | 16.6 | 0.47 | 3.97 | 4.90 | 0.69 | 25.1 | 9.01 | 122 | 44.0 | 208 | 44.5 | 453 | 72.7 | 8663 | 0.80 |
| QK-8-05 | 823 | -0.89 | 23.7 | 131 | 1041 | 0.84 | 0.08 | 8.97 | 0.09 | 1.34 | 2.87 | 0.51 | 17.4 | 6.23 | 90.1 | 31.2 | 156 | 33.1 | 338 | 56.2 | 8633 | 0.49 |
| QK-8-06 | 794 | -0.80 | 17.7 | 98.1 | 965 | 0.90 | 0.01 | 7.05 | 0.08 | 1.26 | 2.54 | 0.49 | 17.1 | 6.11 | 80.0 | 28.9 | 142 | 31.3 | 325 | 54.0 | 8766 | 0.56 |
| QK-8-07 | 801 | -0.52 | 19.0 | 53.7 | 917 | 0.65 | 0.27 | 6.36 | 0.08 | 0.87 | 3.49 | 0.64 | 17.5 | 6.08 | 79.7 | 27.8 | 134 | 27.9 | 281 | 46.9 | 8511 | 0.34 |
| QK-8-08 | 811 | -0.14 | 21.2 | 96.6 | 1392 | 0.72 | 1.39 | 11.2 | 0.59 | 5.18 | 5.91 | 1.11 | 28.1 | 9.47 | 123 | 42.0 | 195 | 41.1 | 415 | 66.5 | 8534 | 0.43 |
| QK-8-09 | 795 | -0.44 | 17.9 | 86.0 | 941 | 0.78 | 0.01 | 8.15 | 0.08 | 1.23 | 3.86 | 0.63 | 17.3 | 5.96 | 83.1 | 27.7 | 136 | 29.7 | 308 | 52.1 | 8394 | 0.41 |

| | | | | | | | | | | | | | | | | | | | | | | |
|---|---|---|---|---|---|---|---|---|---|---|---|---|---|---|---|---|---|---|---|---|---|---|
| QK-8-10 | 781 | -0.29 | 15.5 | 91.9 | 1623 | 0.55 | 0.01 | 8.59 | 0.13 | 3.46 | 6.43 | 1.20 | 34.9 | 10.9 | 143 | 48.6 | 224 | 46.3 | 460 | 74.4 | 8503 | 0.38 |
| QK-8-11 | 776 | -1.11 | 14.8 | 304 | 1733 | 1.42 | 0.01 | 9.48 | 0.12 | 2.16 | 4.62 | 0.87 | 31.8 | 10.4 | 143 | 50.8 | 241 | 50.3 | 502 | 81.7 | 7747 | 0.72 |
| QK-8-12 | 948 | 0.44 | 70.6 | 97.5 | 918 | 1.05 | 9.40 | 28.6 | 3.09 | 16.5 | 5.95 | 0.70 | 19.0 | 6.01 | 78.5 | 27.8 | 136 | 29.4 | 315 | 50.8 | 8281 | 0.47 |
| QK-8-13 | 762 | 0.27 | 12.6 | 91.5 | 832 | 0.78 | 1.08 | 10.6 | 0.36 | 2.90 | 2.65 | 0.40 | 14.3 | 5.20 | 70.1 | 25.3 | 121 | 26.3 | 271 | 46.2 | 8339 | 0.42 |
| QK-8-14 | 790 | -0.10 | 17.1 | 117 | 982 | 0.80 | 1.63 | 11.3 | 0.56 | 3.45 | 3.35 | 0.67 | 18.1 | 6.13 | 81.5 | 29.7 | 144 | 30.7 | 319 | 54.0 | 8372 | 0.47 |
| QK-8-15 | 833 | -0.15 | 26.1 | 436 | 5500 | 3.62 | 0.31 | 26.3 | 0.59 | 8.42 | 21.3 | 5.42 | 126 | 37.9 | 480 | 159 | 722 | 143 | 1339 | 223 | 7026 | 1.20 |
| QK-8-16 | 777 | -0.06 | 14.9 | 84.7 | 936 | 0.84 | 0.21 | 9.19 | 0.12 | 1.34 | 2.67 | 0.51 | 15.5 | 5.66 | 77.1 | 28.3 | 138 | 30.1 | 316 | 55.0 | 8613 | 0.50 |
| QK-8-17 | 795 | -0.78 | 17.9 | 59.8 | 1228 | 0.49 | 0.01 | 5.62 | 0.05 | 1.37 | 4.04 | 0.96 | 25.5 | 8.25 | 113 | 38.0 | 176 | 36.9 | 369 | 60.3 | 8009 | 0.33 |
| QK-8-18 | 769 | -0.41 | 13.6 | 125 | 1517 | 1.02 | 0.013 | 8.72 | 0.11 | 2.46 | 5.03 | 0.93 | 28.2 | 9.60 | 129 | 45.2 | 212 | 44.9 | 463 | 75.6 | 8534 | 0.54 |
| QK-8-19 | 769 | -0.18 | 13.7 | 114 | 936 | 0.86 | 0.17 | 9.54 | 0.13 | 1.28 | 2.70 | 0.51 | 15.8 | 5.85 | 78.9 | 28.3 | 140 | 30.1 | 305 | 52.5 | 8747 | 0.40 |
| QK-8-20 | 804 | -0.86 | 19.6 | 70.1 | 836 | 0.56 | 0.13 | 6.08 | 0.10 | 1.49 | 2.52 | 0.50 | 16.2 | 5.35 | 71.1 | 25.6 | 123 | 26.9 | 279 | 48.0 | 8017 | 0.39 |
| QK-8-21 | 765 | 0.36 | 13.0 | 494 | 3089 | 3.45 | 0.02 | 26.5 | 0.22 | 4.38 | 9.38 | 1.18 | 54.2 | 18.9 | 253 | 88.5 | 414 | 86.7 | 851 | 134 | 8799 | 1.43 |
| QK-8-22 | 755 | -0.36 | 11.7 | 85.8 | 871 | 0.66 | 0.00 | 6.90 | 0.06 | 0.86 | 2.55 | 0.56 | 15.3 | 5.40 | 73.1 | 26.5 | 130 | 27.8 | 297 | 49.9 | 8893 | 0.37 |
| Sample: KM-6 (Basaltic andesite) | | | | | | | | | | | | | | | | | | | | | | |
| KM-6-07 | 739 | 1.33 | 9.79 | 284 | 898 | 1.26 | 0.07 | 30.4 | 0.08 | 1.49 | 2.90 | 1.23 | 16.2 | 5.08 | 65.3 | 24.5 | 128 | 27.9 | 330 | 59.2 | 10183 | 0.42 |
| KM-6-08 | 691 | 2.67 | 5.48 | 187 | 798 | 0.90 | 9.41 | 39.9 | 2.46 | 11.5 | 4.83 | 1.34 | 16.4 | 4.68 | 59.0 | 21.6 | 112 | 25.2 | 296 | 55.8 | 10176 | 0.28 |
| KM-6-09 | 729 | 1.44 | 8.71 | 112 | 604 | 0.62 | 1.01 | 19.2 | 0.23 | 2.46 | 2.87 | 1.01 | 11.8 | 3.58 | 46.4 | 16.3 | 86.4 | 19.4 | 228 | 41.3 | 10211 | 0.26 |
| KM-6-11 | 733 | 1.31 | 9.11 | 116 | 639 | 0.70 | 0.07 | 18.6 | 0.08 | 1.59 | 2.92 | 0.96 | 12.9 | 3.93 | 49.0 | 17.5 | 89.5 | 19.9 | 234 | 42.0 | 10223 | 0.23 |
| KM-6-12 | 677 | 2.98 | 4.59 | 157 | 711 | 0.63 | 8.35 | 40.0 | 2.30 | 11.4 | 5.18 | 1.42 | 16.5 | 4.59 | 56.0 | 19.4 | 100 | 22.3 | 267 | 46.4 | 11223 | 0.33 |
| KM-6-13 | 677 | 1.70 | 4.62 | 230 | 749 | 0.81 | 1.78 | 23.2 | 0.51 | 3.20 | 3.31 | 1.19 | 13.8 | 4.18 | 54.7 | 19.9 | 109 | 24.5 | 299 | 54.0 | 10505 | 0.36 |
| KM-6-14 | 690 | 2.30 | 5.42 | 123 | 698 | 0.66 | 3.22 | 26.2 | 0.88 | 5.62 | 4.35 | 1.27 | 15.7 | 4.54 | 55.9 | 19.3 | 99.7 | 21.9 | 256 | 44.4 | 10391 | 0.28 |
| KM-6-15 | 749 | 1.13 | 10.9 | 96.1 | 656 | 0.66 | 0.07 | 16.7 | 0.09 | 1.43 | 2.86 | 0.96 | 14.0 | 4.08 | 51.6 | 18.6 | 91.9 | 20.3 | 236 | 41.2 | 9955 | 0.25 |
| KM-6-16 | 692 | 1.33 | 5.58 | 134 | 694 | 0.61 | 0.09 | 15.8 | 0.12 | 1.86 | 3.06 | 1.28 | 15.5 | 4.23 | 53.3 | 19.0 | 98.2 | 21.9 | 260 | 45.8 | 9984 | 0.23 |
| KM-6-17 | 721 | 1.35 | 7.94 | 153 | 756 | 0.79 | 0.01 | 20.3 | 0.09 | 1.81 | 3.49 | 1.22 | 14.7 | 4.48 | 55.8 | 20.8 | 107 | 23.6 | 287 | 51.3 | 10132 | 0.34 |
| KM-6-18 | 752 | 0.91 | 11.3 | 111 | 663 | 0.80 | 0.05 | 16.1 | 0.14 | 2.24 | 4.06 | 1.11 | 15.7 | 4.48 | 53.1 | 18.1 | 91.0 | 20.1 | 233 | 41.8 | 9639 | 0.24 |
| KM-6-19 | 728 | 1.75 | 8.64 | 104 | 796 | 0.65 | 2.73 | 22.1 | 0.80 | 5.24 | 4.31 | 1.03 | 18.1 | 5.14 | 63.7 | 21.8 | 112 | 23.4 | 264 | 45.0 | 10195 | 0.26 |
| KM-6-20 | 789 | 3.09 | 16.8 | 176 | 619 | 0.94 | 34.4 | 86.5 | 8.21 | 36.3 | 7.56 | 1.80 | 13.9 | 3.71 | 46.1 | 16.1 | 85.3 | 19.8 | 239 | 44.5 | 9937 | 0.34 |
| KM-6-21 | 718 | 0.37 | 7.67 | 163 | 673 | 0.94 | 0.02 | 11.7 | 0.07 | 1.36 | 2.01 | 1.15 | 12.2 | 3.85 | 48.8 | 18.0 | 94.9 | 21.6 | 263 | 48.2 | 9170 | 0.29 |
| Sample: KM-1 (Dacite) | | | | | | | | | | | | | | | | | | | | | | |
| KM-1-01 | 687 | 1.70 | 5.25 | 470 | 1015 | 2.05 | 3.90 | 35.6 | 0.71 | 3.98 | 2.47 | 0.74 | 14.3 | 5.25 | 71.2 | 28.4 | 150 | 34.9 | 391 | 74.2 | 11406 | 0.84 |
| KM-1-02 | 715 | 2.73 | 7.40 | 479 | 7970 | 4.38 | 0.10 | 77.1 | 1.12 | 21.0 | 37.4 | 10.3 | 167 | 52.1 | 643 | 225 | 1054 | 227 | 2369 | 381 | 8369 | 1.01 |
| KM-1-04 | 739 | 1.21 | 9.83 | 162 | 1185 | 1.47 | 0.01 | 21.4 | 0.08 | 1.30 | 3.36 | 1.22 | 17.5 | 6.07 | 88.2 | 33.6 | 176 | 39.3 | 440 | 77.3 | 9187 | 0.59 |

| | | | | | | | | | | | | | | | | | | | | | | |
|---|---|---|---|---|---|---|---|---|---|---|---|---|---|---|---|---|---|---|---|---|---|---|
| KM-1-05 | 690 | 0.72 | 5.44 | 58.2 | 742 | 0.53 | 0.00 | 7.24 | 0.06 | 1.18 | 2.24 | 1.15 | 11.8 | 3.93 | 50.8 | 20.4 | 110 | 27.8 | 347 | 69.3 | 7431 | 0.19 |
| KM-1-07 | 772 | 1.72 | 14.0 | 130 | 1380 | 1.59 | 0.00 | 30.9 | 0.11 | 2.16 | 4.08 | 1.84 | 24.6 | 8.41 | 108 | 40.0 | 196 | 41.9 | 438 | 73.9 | 8532 | 0.57 |
| KM-1-08 | 687 | 1.99 | 5.25 | 634 | 1070 | 1.63 | 9.95 | 48.6 | 2.25 | 12.2 | 4.96 | 1.93 | 19.6 | 6.69 | 82.5 | 30.9 | 158 | 35.6 | 400 | 73.2 | 9583 | 0.72 |
| KM-1-10 | 690 | 1.47 | 5.45 | 440 | 1449 | 2.88 | 0.02 | 30.7 | 0.05 | 1.18 | 2.80 | 1.05 | 19.0 | 6.73 | 96.8 | 38.9 | 208 | 48.6 | 561 | 101 | 10995 | 1.01 |
| KM-1-11 | 686 | 1.83 | 5.15 | 430 | 1608 | 4.21 | 0.43 | 36.2 | 0.11 | 1.41 | 2.42 | 0.91 | 17.3 | 6.44 | 98.2 | 41.3 | 230 | 55.2 | 627 | 117 | 10863 | 1.35 |
| KM-1-14 | 707 | -0.20 | 6.72 | 76.4 | 318 | 0.27 | 0.01 | 5.42 | 0.03 | 0.28 | 0.66 | 0.43 | 4.18 | 1.44 | 20.2 | 8.68 | 50.9 | 12.7 | 156 | 31.7 | 8366 | 0.13 |
| KM-1-15 | 678 | 1.63 | 4.67 | 464 | 1182 | 2.24 | 0.40 | 32.0 | 0.14 | 1.38 | 2.65 | 0.92 | 16.7 | 5.92 | 85.6 | 33.5 | 177 | 41.4 | 466 | 84.6 | 10865 | 0.95 |
| KM-1-16 | 718 | 1.04 | 7.64 | 130 | 1078 | 1.66 | 0.09 | 15.4 | 0.06 | 1.06 | 2.56 | 0.51 | 16.2 | 5.71 | 79.7 | 31.7 | 162 | 36.8 | 402 | 69.7 | 10932 | 0.74 |
| KM-1-17 | 748 | 1.52 | 10.8 | 121 | 1037 | 1.29 | 0.003 | 23.3 | 0.06 | 1.14 | 2.81 | 0.82 | 17.5 | 6.07 | 81.6 | 30.8 | 155 | 34.3 | 372 | 66.2 | 9511 | 0.55 |
| KM-1-18 | 733 | 3.21 | 9.16 | 375 | 8871 | 5.73 | 0.23 | 100 | 1.97 | 35.1 | 54.3 | 21.3 | 215 | 62.0 | 722 | 241 | 1140 | 250 | 2726 | 470 | 7877 | 0.76 |
| KM-1-19 | 710 | -0.43 | 6.93 | 128 | 928 | 0.48 | 0.01 | 6.25 | 0.11 | 1.51 | 2.78 | 1.54 | 15.0 | 4.88 | 67.4 | 25.8 | 137 | 32.2 | 379 | 72.1 | 8555 | 0.23 |
| KM-1-22 | 727 | 2.20 | 8.52 | 144 | 1053 | 1.44 | 4.65 | 33.3 | 1.35 | 7.45 | 4.59 | 0.99 | 17.8 | 6.15 | 81.6 | 31.8 | 156 | 34.9 | 375 | 63.9 | 10047 | 0.65 |
| Sample: BS-13 (Rhyolite) | | | | | | | | | | | | | | | | | | | | | | |
| BS-13-01 | 706 | 0.69 | 6.65 | 273 | 4141 | 1.79 | 3.04 | 17.0 | 1.51 | 14.0 | 20.6 | 3.40 | 113 | 37.9 | 428 | 155 | 649 | 124 | 1080 | 200 | 7337 | 0.50 |
| BS-13-02 | 748 | 3.34 | 10.9 | 501 | 4213 | 4.39 | 15.4 | 135 | 8.10 | 47.7 | 30.1 | 3.86 | 121 | 38.8 | 439 | 156 | 650 | 126 | 1097 | 200 | 8083 | 1.26 |
| BS-13-03 | 732 | -0.30 | 9.06 | 213 | 1478 | 1.32 | 0.20 | 9.96 | 0.22 | 2.26 | 5.27 | 0.93 | 31.0 | 11.6 | 139 | 53.9 | 231 | 46.5 | 413 | 78.7 | 7311 | 0.52 |
| BS-13-04 | 747 | 2.19 | 10.7 | 1007 | 6466 | 5.94 | 14.0 | 98.6 | 7.07 | 44.7 | 42.3 | 7.51 | 204 | 65.2 | 688 | 231 | 930 | 181 | 1534 | 278 | 9013 | 1.77 |
| BS-13-05 | 720 | 3.19 | 7.79 | 343 | 2862 | 2.45 | 25.3 | 87.2 | 11.3 | 60.2 | 25.4 | 2.41 | 82.6 | 25.5 | 290 | 106 | 445 | 87.1 | 767 | 143 | 7665 | 0.67 |
| BS-13-06 | 734 | 1.09 | 9.18 | 262 | 2244 | 1.32 | 6.23 | 24.6 | 2.96 | 18.9 | 13.2 | 2.05 | 57.8 | 19.0 | 215 | 82.1 | 357 | 71.8 | 638 | 121 | 6951 | 0.50 |
| BS-13-08 | 811 | 1.66 | 21.1 | 297 | 2822 | 2.58 | 1.37 | 55.3 | 1.62 | 14.9 | 17.9 | 2.52 | 79.0 | 25.5 | 282 | 101 | 432 | 85.3 | 743 | 141 | 6770 | 0.87 |
| BS-13-10 | 1101 | 2.30 | 206 | 702 | 4975 | 17.0 | 184 | 384 | 38.6 | 160 | 41.8 | 0.84 | 147 | 47.8 | 549 | 195 | 776 | 141 | 1146 | 193 | 8299 | 2.90 |
| BS-13-12 | 744 | -1.24 | 10.3 | 152 | 1696 | 1.23 | 0.02 | 5.20 | 0.08 | 2.19 | 5.22 | 1.07 | 32.3 | 11.7 | 150 | 59.9 | 274 | 56.8 | 531 | 106 | 7520 | 0.52 |
| BS-13-18 | 730 | 1.50 | 8.77 | 598 | 6616 | 4.79 | 3.49 | 46.2 | 2.21 | 23.0 | 34.4 | 4.87 | 193 | 62.9 | 714 | 249 | 1007 | 193 | 1622 | 291 | 7484 | 1.14 |
| BS-13-19 | 753 | -1.15 | 11.5 | 198 | 2232 | 0.78 | 0.12 | 6.60 | 0.28 | 4.82 | 8.72 | 1.86 | 53.5 | 18.3 | 218 | 79.6 | 348 | 71.6 | 647 | 124 | 7774 | 0.36 |
| BS-13-22 | 741 | -0.99 | 9.96 | 282 | 3384 | 0.78 | 0.04 | 8.03 | 0.35 | 8.06 | 14.2 | 2.71 | 82.6 | 27.0 | 324 | 121 | 521 | 108 | 983 | 188 | 6871 | 0.36 |
| BS-13-23 | 737 | -1.62 | 9.58 | 158 | 1947 | 1.15 | 0.07 | 4.11 | 0.19 | 2.78 | 7.52 | 1.64 | 42.9 | 15.3 | 184 | 71.0 | 311 | 63.8 | 581 | 111 | 6932 | 0.28 |
| BS-13-24 | 662 | 1.52 | 3.78 | 607 | 6024 | 3.59 | 0.05 | 30.9 | 0.56 | 13.2 | 29.8 | 3.92 | 164 | 55.8 | 640 | 228 | 944 | 183 | 1533 | 272 | 8065 | 0.88 |
| BS-13-25 | 723 | -0.04 | 8.08 | 311 | 1986 | 2.41 | 0.13 | 13.2 | 0.19 | 2.52 | 5.97 | 0.90 | 43.6 | 15.1 | 192 | 73.0 | 313 | 62.8 | 566 | 105 | 7915 | 0.73 |
| BS-13-26 | 701 | 0.90 | 6.25 | 414 | 3008 | 2.13 | 0.61 | 23.0 | 0.56 | 6.05 | 13.3 | 2.32 | 71.7 | 25.7 | 297 | 110 | 463 | 90.3 | 804 | 150 | 7092 | 0.65 |
| BS-13-27 | 679 | 0.35 | 4.71 | 236 | 3633 | 1.33 | 0.06 | 11.0 | 0.42 | 8.16 | 18.3 | 3.13 | 104 | 33.7 | 388 | 138 | 571 | 110 | 943 | 173 | 7528 | 0.51 |
| BS-13-28 | 637 | 2.11 | 2.69 | 766 | 3693 | 16.1 | 0.01 | 41.1 | 0.20 | 3.31 | 12.8 | 0.072 | 90.8 | 33.0 | 391 | 143 | 577 | 108 | 891 | 150 | 8499 | 3.47 |
| BS-13-30 | 706 | 1.31 | 6.60 | 581 | 7118 | 3.99 | 2.04 | 35.3 | 1.61 | 17.9 | 32.6 | 4.79 | 198 | 64.9 | 741 | 264 | 1099 | 212 | 1783 | 318 | 7629 | 0.94 |

**Table S3.** Whole-rock $^{40}Ar$-$^{39}Ar$ data for the BJE mafic dikes from the East Junggar.

| Step | Laster power | | $^{36}Ar(a)$ | $^{37}Ar(ca)$ | $^{38}Ar(cl)$ | $^{39}Ar(k)$ | $^{40}Ar(r)$ | Age (Ma) | ±2σ | $^{40}Ar(r)$ (%) | $^{39}Ar(k)$ (%) | K/Ca | ±2σ |
|---|---|---|---|---|---|---|---|---|---|---|---|---|---|
| BJE-8, plateau age=320.4±1.6 Ma, J=0.01057509±0.00002644, $I_0$=295.5. | | | | | | | | | | | | | |
| 16WHA0331-004 | 3.5% | | 7.93032 | 11.70934 | 0.15945 | 142.86892 | 2854.63396 | 346.6 | ±4.6 | 54.9 | 2.82 | 4.722 | ±0.259 |
| 16WHA0331-005 | 4.0% | | 1.30828 | 5.81096 | 0.00000 | 49.55528 | 1022.90507 | 357.0 | ±2.7 | 72.6 | 0.98 | 3.300 | ±0.385 |
| 16WHA0331-006 | 4.5% | | 1.23192 | 18.24484 | 0.02662 | 172.24654 | 3386.21409 | 341.6 | ±1.5 | 90.3 | 3.40 | 3.654 | ±0.248 |
| 16WHA0331-007 | 5.0% | | 0.96944 | 28.31807 | 0.05642 | 245.54418 | 4726.07427 | 335.0 | ±1.4 | 94.3 | 4.85 | 3.356 | ±0.119 |
| 16WHA0331-009 | 5.5% | | 0.36862 | 9.81005 | 0.00000 | 83.79709 | 1620.25063 | 336.4 | ±1.4 | 93.7 | 1.66 | 3.306 | ±0.376 |
| 16WHA0331-010 | 6.0% | | 0.47076 | 26.35622 | 0.00318 | 192.90002 | 3654.69573 | 330.2 | ±1.4 | 96.3 | 3.81 | 2.832 | ±0.225 |
| 16WHA0331-011 | 6.6% | | 0.21545 | 11.77276 | 0.00000 | 94.01076 | 1803.62175 | 334.0 | ±1.5 | 96.6 | 1.86 | 3.090 | ±0.360 |
| 16WHA0331-012 | 7.2% | | 0.20356 | 20.27854 | 0.00000 | 155.06004 | 2938.66917 | 330.3 | ±1.4 | 98.0 | 3.06 | 2.959 | ±0.169 |
| 16WHA0331-013 | 8.0% | # | 0.41186 | 40.43536 | 0.09006 | 301.40274 | 5523.65293 | 320.3 | ±1.3 | 97.8 | 5.95 | 2.885 | ±0.148 |
| 16WHA0331-014 | 8.8% | # | 0.47895 | 42.58021 | 0.15261 | 333.78948 | 6126.98333 | 320.8 | ±1.3 | 97.7 | 6.59 | 3.034 | ±0.149 |
| 16WHA0331-016 | 9.6% | # | 0.38456 | 35.93165 | 0.15078 | 286.54225 | 5258.44334 | 320.7 | ±1.3 | 97.9 | 5.66 | 3.086 | ±0.253 |
| 16WHA0331-017 | 10.6% | # | 0.54331 | 44.59050 | 0.20556 | 333.42554 | 6108.07684 | 320.2 | ±1.2 | 97.4 | 6.59 | 2.894 | ±0.134 |
| 16WHA0331-018 | 12.0% | # | 0.83535 | 67.20224 | 0.34435 | 487.58609 | 8926.62194 | 320.0 | ±1.2 | 97.3 | 9.63 | 2.808 | ±0.093 |
| 16WHA0331-019 | 15.0% | # | 2.55163 | 200.27721 | 1.36638 | 1211.05634 | 22188.40003 | 320.3 | ±1.2 | 96.7 | 23.92 | 2.340 | ±0.159 |
| 16WHA0331-020 | 20.0% | | 3.03238 | 163.73541 | 1.09245 | 639.00502 | 11474.40747 | 314.4 | ±1.3 | 92.7 | 12.62 | 1.510 | ±0.085 |
| 16WHA0331-022 | 25.0% | | 1.80742 | 98.82547 | 0.43158 | 227.97098 | 3952.38059 | 304.4 | ±1.3 | 88.1 | 4.50 | 0.893 | ±0.040 |
| 16WHA0331-023 | 30.0% | | 0.41919 | 26.21646 | 0.00975 | 72.79626 | 1255.87567 | 303.0 | ±1.3 | 91.0 | 1.44 | 1.075 | ±0.045 |
| 16WHA0331-024 | 35.0% | | 0.18983 | 11.58665 | 0.00000 | 32.33311 | 559.08735 | 303.7 | ±1.4 | 90.9 | 0.64 | 1.080 | ±0.074 |
| BJE-9, total fusion age=324.1±1.6 Ma, J=0.01065911±0.00002665, $I_0$=295.5. | | | | | | | | | | | | | |
| 16WHA0332-003 | 3.0% | | 6.81532 | 25.02296 | 0.25772 | 95.98443 | 1865.32773 | 340.4 | ±11.5 | 48.1 | 2.16 | 1.484 | ±0.090 |
| 16WHA0332-004 | 3.5% | | 2.70254 | 25.24538 | 0.22907 | 134.40699 | 2690.36054 | 349.7 | ±7.2 | 77.1 | 3.02 | 2.060 | ±0.125 |
| 16WHA0332-005 | 4.0% | | 0.96145 | 35.19461 | 0.27989 | 257.86231 | 5276.02372 | 356.8 | ±4.6 | 94.9 | 5.80 | 2.835 | ±0.159 |
| 16WHA0332-006 | 4.5% | | 0.35928 | 24.78783 | 0.10601 | 165.88924 | 3430.26020 | 360.2 | ±3.8 | 97.0 | 3.73 | 2.590 | ±0.173 |
| 16WHA0332-007 | 5.0% | | 0.77574 | 93.25611 | 0.55024 | 774.50095 | 14974.80323 | 338.9 | ±1.8 | 98.5 | 17.42 | 3.214 | ±0.195 |
| 16WHA0332-009 | 5.5% | | 0.03940 | 10.51525 | 0.02115 | 131.36736 | 2472.11214 | 330.6 | ±1.4 | 99.5 | 2.95 | 4.835 | ±0.494 |
| 16WHA0332-011 | 6.0% | | 0.00000 | 3.17300 | 0.00000 | 162.72431 | 3024.16830 | 326.8 | ±1.3 | 100.0 | 3.66 | 19.847 | ±5.141 |
| 16WHA0332-012 | 6.6% | | 0.30879 | 35.04097 | 0.22676 | 414.21243 | 7613.32034 | 323.5 | ±1.2 | 98.8 | 9.32 | 4.575 | ±0.204 |
| 16WHA0332-013 | 7.2% | | 0.46153 | 33.28162 | 0.41458 | 525.36964 | 9577.44173 | 321.1 | ±1.2 | 98.6 | 11.82 | 6.109 | ±0.407 |

| | | | | | | | | | | | | |
|---|---|---|---|---|---|---|---|---|---|---|---|---|
| 16WHA0332-014 | 8.0% | 0.22452 | 11.80174 | 0.16365 | 246.75312 | 4452.79612 | 318.1 | ±1.2 | 98.5 | 5.55 | 8.091 | ±0.721 |
| 16WHA0332-015 | 8.8% | 0.33467 | 13.71104 | 0.27115 | 290.68451 | 5207.47262 | 316.0 | ±1.2 | 98.1 | 6.54 | 8.205 | ±0.833 |
| 16WHA0332-017 | 9.6% | 0.38489 | 12.27612 | 0.29235 | 267.92102 | 4774.65826 | 314.5 | ±1.2 | 97.7 | 6.03 | 8.446 | ±0.774 |
| 16WHA0332-018 | 10.6% | 0.47501 | 18.32777 | 0.29339 | 243.53090 | 4274.66612 | 310.1 | ±1.2 | 96.8 | 5.48 | 5.142 | ±0.396 |
| 16WHA0332-019 | 12.0% | 0.60204 | 31.15221 | 0.24834 | 194.26983 | 3341.09002 | 304.4 | ±1.2 | 94.9 | 4.37 | 2.413 | ±0.140 |
| 16WHA0332-020 | 15.0% | 1.37814 | 113.01705 | 0.51515 | 278.16512 | 4618.48883 | 294.7 | ±1.2 | 91.9 | 6.26 | 0.953 | ±0.046 |
| 16WHA0332-021 | 20.0% | 0.87617 | 61.89103 | 0.30711 | 173.39841 | 2844.06553 | 291.4 | ±1.2 | 91.6 | 3.90 | 1.084 | ±0.029 |
| 16WHA0332-022 | 25.0% | 0.39261 | 20.72606 | 0.06756 | 69.30463 | 1121.68694 | 287.8 | ±1.2 | 90.6 | 1.56 | 1.294 | ±0.066 |
| 16WHA0332-023 | 30.0% | 0.16091 | 6.81414 | 0.00000 | 19.68366 | 313.56420 | 283.6 | ±1.6 | 86.8 | 0.44 | 1.118 | ±0.146 |

Data marked with "#" were included in the calculations for the isochron ages.

**Table S4.** Whole-rock major and trace element data for the Carboniferous igneous rocks from the East Junggar.

| Sample No. | QK-1 | QK-2 | QK-3 | QK-4 | QK-5 | QK-6 | QK-7 | QK-8 | KM-1 | KM-2 | KM-3 |
|---|---|---|---|---|---|---|---|---|---|---|---|
| Lithology | Basalt | Basalt | Basaltic andesite | Basaltic andesite | Basaltic andesite | Basaltic andesite | Andesite | Dacite | Dacite | Basalt | Andesite |
| Age | Early Carboniferous (ca. 340 Ma) | | | | | | | | Early Carboniferous (ca. 330 Ma) | | |
| Major element (wt %) | | | | | | | | | | | |
| $SiO_2$ | 51.79 | 51.32 | 52.42 | 52.20 | 52.31 | 53.72 | 60.72 | 64.74 | 63.71 | 50.06 | 58.46 |
| $TiO_2$ | 2.84 | 2.99 | 2.44 | 2.82 | 1.82 | 1.30 | 1.57 | 0.90 | 0.60 | 0.90 | 0.83 |
| $Al_2O_3$ | 14.68 | 15.05 | 15.53 | 14.84 | 14.71 | 15.62 | 16.40 | 15.73 | 16.63 | 18.36 | 15.78 |
| $Fe_2O_3$ | 11.24 | 11.82 | 11.09 | 10.11 | 9.26 | 7.98 | 6.06 | 5.26 | 4.51 | 9.93 | 9.26 |
| MnO | 0.18 | 0.24 | 0.16 | 0.22 | 0.14 | 0.17 | 0.06 | 0.08 | 0.11 | 0.19 | 0.10 |
| MgO | 3.60 | 2.82 | 3.49 | 3.07 | 3.57 | 2.22 | 1.67 | 1.35 | 1.68 | 4.70 | 2.51 |
| CaO | 4.43 | 3.69 | 4.56 | 4.95 | 5.70 | 7.18 | 4.10 | 2.22 | 3.20 | 8.15 | 5.49 |
| $Na_2O$ | 1.16 | 3.54 | 3.26 | 2.31 | 3.15 | 3.67 | 3.55 | 3.38 | 3.82 | 2.72 | 5.34 |
| $K_2O$ | 4.15 | 2.75 | 2.59 | 4.02 | 2.12 | 2.18 | 2.46 | 3.85 | 2.82 | 1.54 | 0.13 |
| $P_2O_5$ | 0.82 | 0.84 | 0.89 | 0.81 | 0.73 | 0.54 | 0.40 | 0.25 | 0.18 | 0.24 | 0.23 |
| LOI | 4.80 | 4.60 | 3.70 | 4.12 | 6.75 | 5.45 | 2.66 | 2.01 | 2.30 | 2.50 | 2.06 |
| Total | 99.67 | 99.65 | 100.12 | 99.46 | 100.25 | 100.03 | 99.65 | 99.77 | 99.56 | 99.27 | 100.18 |
| $Mg^{\#}$ | 39 | 32 | 38 | 38 | 43 | 36 | 35 | 34 | 42 | 48 | 35 |
| Trace element (ppm) | | | | | | | | | | | |
| Sc | 29.1 | 30.3 | 26.5 | 29.6 | 17.5 | 18.0 | 11.7 | 11.1 | 10.1 | 30.9 | 26.4 |
| V | 220 | 184 | 218 | 219 | 162 | 150 | 144 | 67.5 | 81.4 | 291 | 201 |
| Cr | 32.0 | 36.1 | 116 | 34.0 | 22.5 | 53.6 | 121 | 5.67 | 3.67 | 11.8 | 8.70 |
| Co | 28.0 | 29.6 | 37.5 | 33.4 | 26.9 | 24.8 | 24.5 | 17.8 | 13.6 | 35.9 | 42.6 |
| Ni | 5.13 | 6.48 | 29.6 | 5.52 | 23.9 | 25.0 | 56.0 | 5.17 | 5.10 | 17.3 | 14.1 |
| Ga | 20.9 | 19.1 | 19.7 | 19.1 | 19.6 | 18.8 | 16.1 | 21.4 | 17.7 | 18.8 | 11.9 |
| Rb | 96.0 | 57.4 | 3.34 | 84.8 | 54.8 | 29.1 | 12.5 | 88.2 | 64.1 | 22.1 | 1.83 |
| Sr | 292 | 297 | 392 | 609 | 382 | 592 | 669 | 395 | 605 | 631 | 303 |
| Y | 54.9 | 53.8 | 49.7 | 52.8 | 39.8 | 36.0 | 30.4 | 33.9 | 17.6 | 16.6 | 15.6 |
| Zr | 346 | 366 | 324 | 356 | 291 | 327 | 331 | 335 | 173 | 47.4 | 43.5 |

| | | | | | | | | | | | |
|---|---|---|---|---|---|---|---|---|---|---|---|
| Nb | 17.3 | 17.9 | 18.3 | 17.4 | 17.8 | 17.8 | 14.8 | 12.4 | 7.30 | 2.32 | 2.13 |
| Ba | 1369 | 1034 | 180 | 1174 | 480 | 625 | 697 | 550 | 902 | 1055 | 125 |
| La | 32.3 | 35.0 | 33.9 | 33.4 | 35.6 | 40.7 | 30.8 | 28.7 | 21.4 | 8.16 | 7.69 |
| Ce | 74.9 | 82.5 | 81.4 | 78.8 | 76.3 | 84.4 | 64.3 | 62.6 | 43.3 | 19.0 | 17.6 |
| Pr | 10.1 | 11.0 | 10.6 | 10.4 | 9.73 | 10.2 | 7.81 | 7.73 | 5.19 | 2.65 | 2.44 |
| Nd | 43.6 | 47.8 | 46.0 | 45.7 | 40.4 | 41.4 | 32.5 | 30.2 | 20.1 | 12.4 | 11.3 |
| Sm | 10.5 | 10.9 | 10.5 | 10.7 | 8.24 | 8.56 | 7.06 | 6.82 | 4.03 | 3.26 | 2.92 |
| Eu | 3.08 | 3.50 | 2.89 | 2.99 | 2.50 | 2.19 | 1.88 | 1.56 | 1.16 | 1.09 | 1.00 |
| Ti | 17005 | 17946 | 14625 | 16873 | 10891 | 7762 | 9411 | 5395 | 3602 | 5371 | 4993 |
| Gd | 10.8 | 10.8 | 10.0 | 10.9 | 8.00 | 7.54 | 7.09 | 6.27 | 3.54 | 3.19 | 2.97 |
| Tb | 1.75 | 1.67 | 1.55 | 1.67 | 1.21 | 1.15 | 0.85 | 0.99 | 0.54 | 0.49 | 0.46 |
| Dy | 10.2 | 9.64 | 9.03 | 9.86 | 7.05 | 6.54 | 4.88 | 5.89 | 3.05 | 3.03 | 2.83 |
| Ho | 2.09 | 1.93 | 1.83 | 1.98 | 1.45 | 1.32 | 1.09 | 1.21 | 0.60 | 0.62 | 0.56 |
| Er | 5.78 | 5.48 | 5.02 | 5.54 | 4.00 | 3.74 | 3.05 | 3.56 | 1.91 | 1.81 | 1.67 |
| Tm | 0.80 | 0.79 | 0.71 | 0.75 | 0.57 | 0.54 | 0.46 | 0.50 | 0.28 | 0.25 | 0.23 |
| Yb | 5.06 | 5.03 | 4.63 | 5.14 | 3.62 | 3.59 | 2.99 | 3.56 | 1.93 | 1.72 | 1.54 |
| Lu | 0.74 | 0.75 | 0.69 | 0.76 | 0.56 | 0.52 | 0.46 | 0.52 | 0.30 | 0.26 | 0.24 |
| Hf | 7.89 | 8.36 | 7.15 | 8.10 | 6.43 | 7.41 | 7.06 | 8.32 | 4.41 | 1.39 | 1.27 |
| Ta | 1.10 | 1.14 | 0.99 | 1.14 | 1.16 | 0.92 | 1.55 | 1.02 | 0.49 | 0.14 | 0.18 |
| K | 34461 | 22852 | 21491 | 33316 | 17550 | 18106 | 20413 | 31963 | 23417 | 12795 | 1112 |
| Pb | 38.5 | 10.2 | 5.76 | 9.81 | 20.6 | 13.1 | 7.16 | 12.2 | 15.6 | 4.60 | 2.62 |
| Th | 2.94 | 2.97 | 1.35 | 3.01 | 5.05 | 3.20 | 2.80 | 9.88 | 4.88 | 0.83 | 0.77 |
| U | 1.50 | 1.55 | 0.90 | 1.84 | 1.87 | 1.18 | 1.25 | 3.10 | 1.59 | 0.46 | 0.25 |
| $(La/Yb)_N$ | 4.59 | 4.99 | 5.24 | 4.66 | 7.06 | 8.13 | 7.40 | 5.79 | 7.93 | 3.41 | 3.57 |
| ∑REE | 212 | 227 | 219 | 219 | 199 | 212 | 165 | 160 | 107 | 57.9 | 53.5 |
| Eu* | 0.89 | 0.98 | 0.86 | 0.84 | 0.94 | 0.83 | 0.81 | 0.73 | 0.94 | 1.04 | 1.04 |

**Table S4** (continued)

| Sample No. | KM-4 | KM-5 | KM-6 | BJE-1 | BJE-2 | BJE-3 | BJE-4 | BJE-6 | BJE-7 | BJE-8 | BJE-9 |
|---|---|---|---|---|---|---|---|---|---|---|---|
| Lithology | Andesite | Basaltic andesite | Basaltic andesite | Dioritic porphyry | Diabase | Diabase | Dioritic porphyry | Diabase | Diabase | Diabase | Diabase |
| Age | Early Carboniferous (ca. 330 Ma) | | | Late Carboniferous (ca. 320 Ma) | | | | | | | |
| Major element (wt %) | | | | | | | | | | | |
| $SiO_2$ | 60.16 | 54.55 | 52.84 | 55.60 | 52.00 | 52.20 | 55.90 | 48.20 | 47.30 | 52.51 | 51.90 |
| $TiO_2$ | 0.62 | 0.75 | 1.23 | 1.15 | 2.34 | 2.14 | 1.11 | 2.88 | 3.03 | 2.33 | 2.29 |
| $Al_2O_3$ | 17.16 | 17.58 | 17.43 | 16.10 | 13.90 | 14.00 | 15.90 | 13.40 | 13.40 | 13.31 | 13.56 |
| $Fe_2O_3$ | 4.95 | 9.32 | 9.17 | 7.84 | 11.08 | 11.44 | 7.33 | 13.22 | 13.00 | 11.34 | 11.30 |
| MnO | 0.08 | 0.15 | 0.15 | 0.08 | 0.18 | 0.32 | 0.12 | 0.21 | 0.26 | 0.23 | 0.23 |
| MgO | 3.37 | 3.86 | 4.13 | 2.23 | 2.84 | 2.45 | 2.14 | 3.76 | 2.84 | 2.53 | 2.58 |
| CaO | 5.69 | 7.84 | 6.62 | 6.57 | 6.15 | 6.10 | 7.82 | 7.80 | 8.06 | 6.73 | 6.81 |
| $Na_2O$ | 4.34 | 3.26 | 4.02 | 2.58 | 3.59 | 3.52 | 3.38 | 2.92 | 2.96 | 3.12 | 3.09 |
| $K_2O$ | 1.14 | 0.80 | 1.19 | 1.57 | 0.75 | 1.53 | 1.38 | 0.79 | 1.08 | 1.20 | 1.21 |
| $P_2O_5$ | 0.20 | 0.20 | 0.35 | 0.43 | 1.09 | 0.99 | 0.44 | 0.74 | 0.72 | 0.95 | 0.97 |
| LOI | 1.46 | 1.38 | 2.46 | 5.98 | 6.08 | 5.12 | 4.48 | 5.88 | 6.83 | 5.52 | 6.06 |
| Total | 99.15 | 99.68 | 99.58 | 100.13 | 100.00 | 99.81 | 100.00 | 99.80 | 99.48 | 99.78 | 99.98 |
| $Mg^{\#}$ | 57 | 45 | 47 | 36 | 34 | 30 | 37 | 36 | 30 | 31 | 31 |
| Trace element (ppm) | | | | | | | | | | | |
| Sc | 12.2 | 21.7 | 22.2 | 17.3 | 32.3 | 37.3 | 13.8 | 42.5 | 38.9 | 40.4 | 36.3 |
| V | 107 | 215 | 230 | 148 | 141 | 103 | 119 | 341 | 319 | 114 | 136 |
| Cr | 54.7 | 7.82 | 18.5 | 85.5 | 7.17 | 5.49 | 71.6 | 6.94 | 8.75 | 1.42 | 1.39 |
| Co | 32.8 | 54.3 | 32.1 | 22.2 | 13.7 | 10.9 | 19.8 | 28.6 | 26.9 | 52.9 | 45.5 |
| Ni | 43.1 | 14.5 | 16.9 | 49.6 | 1.10 | 1.59 | 35.4 | 5.69 | 5.75 | 22.7 | 17.9 |
| Ga | 19.3 | 17.5 | 19.1 | 19.7 | 21.0 | 19.0 | 16.3 | 21.1 | 19.6 | 21.3 | 20.4 |
| Rb | 16.8 | 12.6 | 24.5 | 32.0 | 17.8 | 18.8 | 20.0 | 10.7 | 15.5 | 13.8 | 19.3 |
| Sr | 942 | 653 | 901 | 502 | 476 | 455 | 560 | 452 | 434 | 489 | 556 |
| Y | 9.62 | 15.3 | 20.7 | 24.8 | 56.8 | 50.9 | 20.2 | 50.8 | 45.8 | 56.5 | 57.5 |
| Zr | 114 | 48.2 | 113 | 242 | 278 | 258 | 207 | 245 | 223 | 322 | 307 |

| | | | | | | | | | | | |
|---|---|---|---|---|---|---|---|---|---|---|---|
| Nb | 3.00 | 2.14 | 5.98 | 10.3 | 12.2 | 11.4 | 9.04 | 10.3 | 9.40 | 12.2 | 11.6 |
| Ba | 399 | 386 | 361 | 332 | 142 | 438 | 472 | 263 | 250 | 347 | 554 |
| La | 14.0 | 7.02 | 16.2 | 29.9 | 24.3 | 23.8 | 25.9 | 21.3 | 19.7 | 25.2 | 25.5 |
| Ce | 29.4 | 16.7 | 38.4 | 63.5 | 64.8 | 61.6 | 55.3 | 54.0 | 50.3 | 63.9 | 63.7 |
| Pr | 3.37 | 2.41 | 5.31 | 7.99 | 9.01 | 8.67 | 6.85 | 7.79 | 7.09 | 9.15 | 9.11 |
| Nd | 13.4 | 11.3 | 23.7 | 31.5 | 41.4 | 37.5 | 27.1 | 35.2 | 32.9 | 42.4 | 42.2 |
| Sm | 2.62 | 2.90 | 5.52 | 6.22 | 10.5 | 9.67 | 5.65 | 9.10 | 8.59 | 10.6 | 10.6 |
| Eu | 0.88 | 0.99 | 1.62 | 1.65 | 3.49 | 3.57 | 1.44 | 2.94 | 2.70 | 3.83 | 3.62 |
| Ti | 3710 | 4501 | 7361 | 6893 | 14026 | 12827 | 6653 | 17263 | 18162 | 13936 | 13720 |
| Gd | 2.31 | 2.94 | 4.88 | 5.67 | 11.1 | 10.3 | 4.70 | 9.47 | 8.60 | 10.9 | 11.0 |
| Tb | 0.35 | 0.46 | 0.71 | 0.79 | 1.67 | 1.50 | 0.65 | 1.44 | 1.35 | 1.72 | 1.73 |
| Dy | 1.84 | 2.73 | 3.95 | 4.52 | 10.1 | 9.03 | 3.76 | 8.81 | 8.08 | 10.2 | 10.2 |
| Ho | 0.35 | 0.56 | 0.76 | 0.93 | 2.14 | 1.94 | 0.76 | 1.86 | 1.69 | 2.04 | 2.05 |
| Er | 0.96 | 1.63 | 1.99 | 2.43 | 5.50 | 5.38 | 1.96 | 4.86 | 4.41 | 5.61 | 5.62 |
| Tm | 0.13 | 0.24 | 0.28 | 0.38 | 0.85 | 0.78 | 0.31 | 0.72 | 0.67 | 0.84 | 0.83 |
| Yb | 0.90 | 1.64 | 1.80 | 2.27 | 5.21 | 4.58 | 1.85 | 4.45 | 4.12 | 5.12 | 4.99 |
| Lu | 0.13 | 0.24 | 0.26 | 0.35 | 0.79 | 0.73 | 0.27 | 0.66 | 0.61 | 0.79 | 0.77 |
| Hf | 2.93 | 1.40 | 2.99 | 5.24 | 6.32 | 5.76 | 4.56 | 5.28 | 4.97 | 6.50 | 6.24 |
| Ta | 0.25 | 0.17 | 0.36 | 0.63 | 0.81 | 0.74 | 0.58 | 0.64 | 0.59 | 1.22 | 1.08 |
| K | 9460 | 6663 | 9891 | 13028 | 6223 | 12696 | 11451 | 6555 | 8962 | 9974 | 9999 |
| Pb | 3.07 | 4.71 | 5.80 | 11.4 | 6.31 | 8.93 | 9.79 | 5.69 | 5.24 | 7.06 | 7.02 |
| Th | 2.45 | 0.61 | 1.83 | 4.42 | 3.22 | 3.19 | 4.02 | 2.03 | 1.90 | 3.25 | 3.07 |
| U | 0.83 | 0.26 | 0.89 | 1.16 | 1.03 | 0.99 | 1.07 | 0.64 | 0.58 | 1.05 | 1.00 |
| $(La/Yb)_N$ | 11.1 | 3.07 | 6.47 | 9.45 | 3.35 | 3.73 | 10.0 | 3.43 | 3.43 | 3.53 | 3.67 |
| ∑REE | 70.6 | 51.8 | 105 | 158 | 191 | 179 | 137 | 163 | 151 | 192 | 192 |
| Eu* | 1.10 | 1.03 | 0.96 | 0.85 | 0.99 | 1.09 | 0.85 | 0.97 | 0.96 | 1.09 | 1.02 |

**Table S4** (continued)

| Sample No. | BS-1 | BS-2 | BS-3 | BS-8 | BS-9 | BS-10 | BS-11 | BS-12 | BS-13 | BS-14 | BS-15 |
|---|---|---|---|---|---|---|---|---|---|---|---|
| Lithology | Dacite | Dacite | Dacite | Rhyolite | Dacite | Dacite | Dacite | Dacite | Rhyolite | Rhyolite | Rhyolite |
| Age | Late Carboniferous (ca. 305 Ma) | | | | | | | | | | |
| Major element (wt %) | | | | | | | | | | | |
| $SiO_2$ | 61.43 | 63.17 | 67.38 | 77.53 | 67.11 | 67.08 | 65.28 | 62.02 | 74.22 | 72.90 | 73.44 |
| $TiO_2$ | 0.60 | 0.48 | 0.58 | 0.17 | 0.51 | 0.41 | 1.17 | 1.10 | 0.10 | 0.12 | 0.14 |
| $Al_2O_3$ | 17.25 | 15.91 | 14.82 | 11.09 | 14.07 | 14.69 | 15.31 | 14.60 | 12.33 | 12.65 | 12.96 |
| $Fe_2O_3$ | 4.83 | 3.76 | 4.09 | 2.19 | 3.87 | 4.26 | 4.76 | 5.50 | 1.54 | 1.80 | 2.02 |
| MnO | 0.08 | 0.07 | 0.07 | 0.07 | 0.05 | 0.06 | 0.04 | 0.08 | 0.02 | 0.02 | 0.03 |
| MgO | 1.38 | 1.60 | 1.18 | 0.03 | 0.94 | 0.33 | 1.10 | 1.23 | 0.10 | 0.12 | 0.09 |
| CaO | 4.02 | 3.42 | 2.23 | 0.12 | 1.88 | 1.50 | 1.00 | 3.11 | 0.75 | 0.75 | 0.43 |
| $Na_2O$ | 3.97 | 4.36 | 3.79 | 3.85 | 4.58 | 4.16 | 4.76 | 4.48 | 4.48 | 4.54 | 4.17 |
| $K_2O$ | 3.25 | 3.01 | 3.52 | 4.29 | 4.44 | 5.59 | 4.16 | 4.01 | 4.81 | 5.14 | 5.41 |
| $P_2O_5$ | 0.19 | 0.14 | 0.15 | 0.01 | 0.08 | 0.08 | 0.30 | 0.29 | 0.02 | 0.02 | 0.02 |
| LOI | 2.99 | 4.00 | 2.16 | 0.62 | 2.55 | 1.80 | 2.58 | 3.88 | 1.32 | 1.64 | 1.07 |
| Total | 99.99 | 99.92 | 99.97 | 99.97 | 100.08 | 99.96 | 100.46 | 100.30 | 99.69 | 99.70 | 99.78 |
| $Mg^{\#}$ | 36 | 46 | 36 | 2.6 | 32 | 13 | 31 | 31 | 11 | 12 | 8.1 |
| Trace element (ppm) | | | | | | | | | | | |
| Sc | 9.21 | 7.79 | 8.85 | 1.20 | 8.99 | 11.7 | 13.1 | 12.4 | 2.87 | 3.98 | 2.91 |
| V | 26.2 | 36.1 | 55.6 | 3.06 | 43.6 | 11.0 | 97.4 | 96.2 | 3.39 | 13.4 | 12.9 |
| Cr | 8.72 | 60.7 | 14.1 | 2.24 | 37.15 | 3.13 | 3.03 | 3.64 | 2.13 | 5.36 | 2.40 |
| Co | 24.3 | 24.4 | 18.4 | 43.2 | 22.4 | 16.2 | 25.5 | 19.3 | 40.9 | 40.7 | 32.6 |
| Ni | 4.19 | 27.4 | 6.75 | 0.9 | 8.67 | 1.32 | 2.3 | 1.49 | 0.94 | 1.11 | 0.88 |
| Ga | 18.5 | 17.6 | 17.1 | 26.8 | 21.6 | 21.2 | 19.1 | 17.8 | 19.5 | 20.9 | 17.1 |
| Rb | 65.8 | 59.5 | 87.0 | 130 | 123 | 99.1 | 97.4 | 88.1 | 109 | 129 | 137 |
| Sr | 506 | 483 | 350 | 52.8 | 111 | 88.7 | 394 | 300 | 70.2 | 160 | 66.2 |
| Y | 19.1 | 12.5 | 30.9 | 93.3 | 52.1 | 41.9 | 30.7 | 39.9 | 26.1 | 33.6 | 30.0 |
| Zr | 159 | 157 | 214 | 642 | 313 | 490 | 316 | 304 | 148 | 211 | 166 |

| | | | | | | | | | | | |
|---|---|---|---|---|---|---|---|---|---|---|---|
| Nb | 6.42 | 6.36 | 7.08 | 16.88 | 9.55 | 8.97 | 9.22 | 8.79 | 4.50 | 6.22 | 5.31 |
| Ba | 1013 | 1301 | 641 | 26.0 | 668 | 1033 | 762 | 675 | 298 | 395 | 573 |
| La | 19.3 | 20.3 | 20.9 | 50.5 | 29.8 | 24.0 | 21.6 | 26.0 | 27.0 | 30.0 | 26.1 |
| Ce | 40.3 | 40.0 | 45.1 | 108 | 67.7 | 53.3 | 52.3 | 56.0 | 55.8 | 63.9 | 54.4 |
| Pr | 4.71 | 4.41 | 5.49 | 13.8 | 8.39 | 6.75 | 6.21 | 7.24 | 6.61 | 7.88 | 6.49 |
| Nd | 18.4 | 16.2 | 21.4 | 56.3 | 32.9 | 27.7 | 25.8 | 29.6 | 24.4 | 29.9 | 23.8 |
| Sm | 3.82 | 3.1 | 4.93 | 13.6 | 7.76 | 6.65 | 5.80 | 6.78 | 5.11 | 6.52 | 5.08 |
| Eu | 1.14 | 0.99 | 1.00 | 0.25 | 0.66 | 0.78 | 0.91 | 1.25 | 0.46 | 0.61 | 0.40 |
| Ti | 3596 | 2877 | 3477 | 1019 | 3057 | 2458 | 7013 | 6593 | 599 | 719 | 839 |
| Gd | 3.45 | 2.62 | 4.84 | 14.0 | 7.80 | 6.57 | 5.66 | 6.71 | 4.50 | 5.79 | 4.83 |
| Tb | 0.53 | 0.38 | 0.8 | 2.46 | 1.32 | 1.08 | 0.88 | 1.06 | 0.69 | 0.91 | 0.81 |
| Dy | 3.10 | 2.10 | 4.95 | 15.23 | 8.21 | 6.64 | 5.16 | 6.36 | 3.99 | 5.48 | 4.93 |
| Ho | 0.65 | 0.43 | 1.06 | 3.30 | 1.79 | 1.42 | 1.11 | 1.37 | 0.89 | 1.18 | 1.05 |
| Er | 1.86 | 1.20 | 3.20 | 9.51 | 5.11 | 4.20 | 3.17 | 3.89 | 2.76 | 3.51 | 3.09 |
| Tm | 0.29 | 0.20 | 0.52 | 1.55 | 0.86 | 0.71 | 0.52 | 0.64 | 0.49 | 0.65 | 0.53 |
| Yb | 1.87 | 1.31 | 3.43 | 9.73 | 5.33 | 4.49 | 3.24 | 4.08 | 3.39 | 3.97 | 3.31 |
| Lu | 0.30 | 0.20 | 0.52 | 1.43 | 0.81 | 0.72 | 0.49 | 0.61 | 0.52 | 0.62 | 0.49 |
| Hf | 4.27 | 4.14 | 5.73 | 17.0 | 8.79 | 9.94 | 7.70 | 7.53 | 4.83 | 6.77 | 5.47 |
| Ta | 0.49 | 0.55 | 0.62 | 1.31 | 0.73 | 0.61 | 0.64 | 0.59 | 0.66 | 0.77 | 0.72 |
| K | 26968 | 24977 | 29209 | 35598 | 36843 | 46385 | 34519 | 33274 | 39913 | 42651 | 44891 |
| Pb | 16.7 | 18.1 | 11.2 | 16.8 | 14.2 | 13.0 | 9.72 | 11.0 | 16.5 | 23.6 | 18.0 |
| Th | 6.70 | 7.18 | 7.45 | 14.03 | 9.25 | 6.78 | 5.62 | 5.51 | 13.14 | 12.29 | 14.06 |
| U | 2.13 | 2.30 | 2.12 | 5.34 | 2.93 | 2.50 | 2.62 | 2.04 | 1.64 | 2.83 | 3.59 |
| $(La/Yb)_N$ | 7.41 | 11.09 | 4.37 | 3.72 | 4.01 | 3.83 | 4.78 | 4.57 | 5.70 | 5.42 | 5.65 |
| ∑REE | 99.8 | 93.3 | 118 | 300 | 178 | 145 | 133 | 152 | 137 | 161 | 135 |
| Eu* | 0.96 | 1.06 | 0.63 | 0.06 | 0.26 | 0.36 | 0.49 | 0.57 | 0.29 | 0.30 | 0.25 |

Mg#=(100MgO/40.31)/(MgO/40.31+0.8998*$Fe_2O_3$/71.85); $Eu^*=Eu_N/(Sm_N \times Gd_N)^{1/2}$, where subscript N denotes chondrite normalization.

**Table S5.** Zircon Hf isotope data for the Carboniferous volcanic rocks from the East Junggar.

| Analytical No. | $^{176}Hf/^{177}Hf$ | 1σ | $^{176}Lu/^{177}Hf$ | 1σ | $^{176}Yb/^{177}Hf$ | 1σ | Age (Ma) | $(^{176}Hf/^{177}Hf)_i$ | $\varepsilon_{Hf}(t)$ | 1σ | $T_{DM}$ (Ma) | 1σ | $T_{crust}$ (Ma) | 1σ |
|---|---|---|---|---|---|---|---|---|---|---|---|---|---|---|
| Sample: QK-7 (Andesite) | | | | | | | | | | | | | | |
| QK-7-03 | 0.281382 | 0.000019 | 0.000798 | 0.000028 | 0.019997 | 0.000746 | 2389 | 0.281345 | 3.1 | 0.7 | 2600 | 26 | 2743 | 44 |
| QK-7-04 | 0.282889 | 0.000032 | 0.001006 | 0.000015 | 0.025877 | 0.000472 | 371 | 0.282882 | 12.1 | 1.1 | 515 | 46 | 602 | 73 |
| QK-7-05 | 0.281417 | 0.000031 | 0.000467 | 0.000009 | 0.010796 | 0.000226 | 2383 | 0.281396 | 4.7 | 1.1 | 2530 | 42 | 2631 | 70 |
| QK-7-07 | 0.282945 | 0.000019 | 0.000992 | 0.000007 | 0.026049 | 0.000214 | 340 | 0.282938 | 13.4 | 0.7 | 436 | 27 | 494 | 43 |
| QK-7-08 | 0.282907 | 0.000022 | 0.000898 | 0.000007 | 0.022204 | 0.000221 | 340 | 0.282901 | 12.0 | 0.8 | 488 | 31 | 579 | 51 |
| QK-7-09 | 0.282328 | 0.000021 | 0.000739 | 0.000004 | 0.017400 | 0.000102 | 474 | 0.282322 | -5.5 | 0.7 | 1296 | 29 | 1803 | 47 |
| QK-7-11 | 0.282955 | 0.000019 | 0.001079 | 0.000005 | 0.027502 | 0.000163 | 340 | 0.282948 | 13.7 | 0.7 | 422 | 28 | 472 | 44 |
| QK-7-12 | 0.281386 | 0.000024 | 0.000675 | 0.000005 | 0.016852 | 0.000134 | 2350 | 0.281355 | 2.5 | 0.9 | 2586 | 33 | 2748 | 55 |
| QK-7-15 | 0.282954 | 0.000022 | 0.001044 | 0.000010 | 0.026704 | 0.000267 | 340 | 0.282948 | 13.7 | 0.8 | 423 | 32 | 473 | 51 |
| QK-7-16 | 0.282936 | 0.000024 | 0.002311 | 0.000013 | 0.060050 | 0.000160 | 340 | 0.282922 | 12.8 | 0.8 | 464 | 35 | 532 | 55 |
| QK-7-17 | 0.282936 | 0.000024 | 0.002311 | 0.000013 | 0.060050 | 0.000160 | 340 | 0.282922 | 12.8 | 0.8 | 464 | 35 | 532 | 55 |
| QK-7-18 | 0.281281 | 0.000037 | 0.000611 | 0.000002 | 0.014677 | 0.000077 | 2421 | 0.281253 | 0.5 | 1.3 | 2724 | 50 | 2932 | 84 |
| QK-7-21 | 0.281338 | 0.000021 | 0.000669 | 0.000009 | 0.016251 | 0.000245 | 2439 | 0.281307 | 2.8 | 0.7 | 2650 | 28 | 2795 | 48 |
| QK-7-22 | 0.282627 | 0.000021 | 0.001210 | 0.000015 | 0.031556 | 0.000756 | 474 | 0.282616 | 4.9 | 0.7 | 891 | 30 | 1141 | 47 |
| Sample: QK-8 (Dacite) | | | | | | | | | | | | | | |
| QK-8-01 | 0.282900 | 0.000019 | 0.000815 | 0.000003 | 0.020472 | 0.000047 | 340 | 0.282895 | 11.8 | 0.7 | 497 | 27 | 594 | 43 |
| QK-8-02 | 0.282937 | 0.000029 | 0.001053 | 0.000015 | 0.026593 | 0.000459 | 340 | 0.282930 | 13.1 | 1.0 | 448 | 41 | 513 | 66 |
| QK-8-03 | 0.282900 | 0.000014 | 0.000703 | 0.000002 | 0.018016 | 0.000044 | 340 | 0.282896 | 11.9 | 0.5 | 495 | 19 | 591 | 31 |
| QK-8-04 | 0.282921 | 0.000022 | 0.000944 | 0.000014 | 0.024118 | 0.000399 | 340 | 0.282915 | 12.5 | 0.8 | 468 | 32 | 547 | 51 |
| QK-8-06 | 0.282908 | 0.000015 | 0.001066 | 0.000010 | 0.027332 | 0.000251 | 340 | 0.282901 | 12.1 | 0.5 | 489 | 22 | 579 | 35 |
| QK-8-07 | 0.282949 | 0.000022 | 0.000625 | 0.000004 | 0.015846 | 0.000099 | 340 | 0.282945 | 13.6 | 0.8 | 425 | 31 | 479 | 50 |
| QK-8-08 | 0.282938 | 0.000023 | 0.001350 | 0.000006 | 0.035474 | 0.000202 | 340 | 0.282930 | 13.1 | 0.8 | 449 | 34 | 514 | 53 |
| QK-8-09 | 0.282919 | 0.000020 | 0.001445 | 0.000011 | 0.038344 | 0.000272 | 340 | 0.282910 | 12.3 | 0.7 | 478 | 28 | 560 | 45 |
| QK-8-10 | 0.282984 | 0.000024 | 0.001152 | 0.000012 | 0.029648 | 0.000347 | 340 | 0.282977 | 14.7 | 0.8 | 382 | 34 | 407 | 54 |
| QK-8-11 | 0.282972 | 0.000024 | 0.001516 | 0.000032 | 0.038902 | 0.000917 | 340 | 0.282963 | 14.2 | 0.9 | 402 | 35 | 438 | 56 |
| QK-8-12 | 0.282921 | 0.000023 | 0.000771 | 0.000018 | 0.019393 | 0.000497 | 340 | 0.282916 | 12.6 | 0.8 | 467 | 32 | 545 | 52 |
| QK-8-13 | 0.282913 | 0.000020 | 0.001233 | 0.000030 | 0.030125 | 0.000650 | 340 | 0.282905 | 12.2 | 0.7 | 484 | 29 | 570 | 46 |
| QK-8-14 | 0.282940 | 0.000028 | 0.000835 | 0.000004 | 0.021244 | 0.000151 | 340 | 0.282935 | 13.2 | 1.0 | 440 | 39 | 502 | 63 |

| | | | | | | | | | | | | | | |
|---|---|---|---|---|---|---|---|---|---|---|---|---|---|---|
| QK-8-15 | 0.283019 | 0.000019 | 0.003363 | 0.000118 | 0.090229 | 0.002989 | 340 | 0.282998 | 15.5 | 0.7 | 352 | 30 | 358 | 45 |
| QK-8-16 | 0.282913 | 0.000019 | 0.001061 | 0.000008 | 0.026087 | 0.000167 | 340 | 0.282906 | 12.2 | 0.7 | 482 | 26 | 567 | 42 |
| QK-8-17 | 0.282912 | 0.000027 | 0.001053 | 0.000009 | 0.026984 | 0.000328 | 340 | 0.282906 | 12.2 | 1.0 | 483 | 39 | 569 | 62 |
| QK-8-18 | 0.283014 | 0.000022 | 0.001296 | 0.000019 | 0.033017 | 0.000495 | 340 | 0.283006 | 15.7 | 0.8 | 340 | 32 | 340 | 51 |
| QK-8-19 | 0.282947 | 0.000025 | 0.000829 | 0.000007 | 0.020592 | 0.000228 | 340 | 0.282942 | 13.5 | 0.9 | 431 | 35 | 487 | 57 |
| QK-8-20 | 0.282927 | 0.000021 | 0.000876 | 0.000006 | 0.021354 | 0.000197 | 340 | 0.282921 | 12.8 | 0.7 | 460 | 30 | 533 | 48 |
| QK-8-21 | 0.282967 | 0.000023 | 0.003003 | 0.000072 | 0.080740 | 0.002281 | 340 | 0.282948 | 13.7 | 0.8 | 426 | 35 | 471 | 54 |
| QK-8-22 | 0.283024 | 0.000024 | 0.000912 | 0.000006 | 0.023107 | 0.000175 | 340 | 0.283019 | 16.2 | 0.9 | 322 | 35 | 311 | 56 |
| Sample: KM-1 (Dacite) | | | | | | | | | | | | | | |
| KM-1-01 | 0.283006 | 0.000014 | 0.001065 | 0.000021 | 0.023962 | 0.000450 | 328 | 0.282999 | 15.3 | 0.5 | 350 | 20 | 363 | 32 |
| KM-1-02 | 0.283077 | 0.000025 | 0.006763 | 0.000054 | 0.165062 | 0.001447 | 328 | 0.283036 | 16.6 | 0.9 | 292 | 43 | 279 | 58 |
| KM-1-04 | 0.283017 | 0.000023 | 0.001547 | 0.000014 | 0.036111 | 0.000373 | 328 | 0.283007 | 15.5 | 0.8 | 338 | 33 | 345 | 53 |
| KM-1-05 | 0.283038 | 0.000018 | 0.001774 | 0.000017 | 0.036377 | 0.000358 | 328 | 0.283027 | 16.2 | 0.6 | 309 | 26 | 298 | 40 |
| KM-1-07 | 0.283033 | 0.000020 | 0.001206 | 0.000022 | 0.028334 | 0.000502 | 328 | 0.283026 | 16.2 | 0.7 | 312 | 28 | 302 | 45 |
| KM-1-08 | 0.283011 | 0.000023 | 0.001349 | 0.000014 | 0.029816 | 0.000334 | 328 | 0.283002 | 15.4 | 0.8 | 345 | 34 | 355 | 54 |
| KM-1-10 | 0.282939 | 0.000019 | 0.001284 | 0.000020 | 0.026760 | 0.000473 | 328 | 0.282931 | 12.8 | 0.7 | 448 | 27 | 519 | 43 |
| KM-1-11 | 0.283023 | 0.000020 | 0.001927 | 0.000029 | 0.040816 | 0.000616 | 328 | 0.283011 | 15.7 | 0.7 | 332 | 29 | 335 | 46 |
| KM-1-14 | 0.282999 | 0.000020 | 0.000519 | 0.000011 | 0.010427 | 0.000229 | 328 | 0.282996 | 15.1 | 0.7 | 354 | 29 | 370 | 47 |
| KM-1-15 | 0.282972 | 0.000018 | 0.001782 | 0.000018 | 0.036867 | 0.000442 | 328 | 0.282961 | 13.9 | 0.6 | 406 | 26 | 451 | 40 |
| KM-1-16 | 0.283077 | 0.000024 | 0.000892 | 0.000011 | 0.020318 | 0.000242 | 328 | 0.283071 | 17.8 | 0.9 | 247 | 35 | 198 | 56 |
| KM-1-17 | 0.283016 | 0.000022 | 0.001202 | 0.000008 | 0.028283 | 0.000258 | 328 | 0.283009 | 15.6 | 0.8 | 336 | 31 | 341 | 50 |
| KM-1-18 | 0.283111 | 0.000027 | 0.008499 | 0.000057 | 0.199140 | 0.001508 | 328 | 0.283058 | 17.3 | 1.0 | 250 | 49 | 227 | 63 |
| KM-1-19 | 0.283107 | 0.000037 | 0.001172 | 0.000011 | 0.024796 | 0.000345 | 328 | 0.283100 | 18.8 | 1.3 | 205 | 53 | 132 | 85 |
| KM-1-22 | 0.283001 | 0.000022 | 0.001011 | 0.000008 | 0.023394 | 0.000221 | 328 | 0.282994 | 15.1 | 0.8 | 356 | 31 | 374 | 51 |
| Sample: BS-13 (Rhyolite) | | | | | | | | | | | | | | |
| BS13-02 | 0.283135 | 0.000015 | 0.004643 | 0.000025 | 0.176025 | 0.000987 | 305 | 0.283108 | 18.6 | 0.5 | 183 | 206 | 127 | 34 |
| BS13-03 | 0.282991 | 0.000015 | 0.002473 | 0.000015 | 0.091465 | 0.000564 | 305 | 0.282977 | 14.0 | 0.5 | 385 | 407 | 428 | 34 |
| BS13-04 | 0.283028 | 0.000019 | 0.004861 | 0.000023 | 0.180874 | 0.000789 | 305 | 0.283001 | 14.8 | 0.7 | 353 | 383 | 375 | 43 |
| BS13-05 | 0.283028 | 0.000013 | 0.003153 | 0.000003 | 0.113749 | 0.000128 | 305 | 0.283010 | 15.1 | 0.5 | 336 | 356 | 352 | 30 |
| BS13-06 | 0.283025 | 0.000014 | 0.002936 | 0.000007 | 0.104064 | 0.000254 | 305 | 0.283009 | 15.1 | 0.5 | 339 | 360 | 356 | 32 |
| BS13-08 | 0.283045 | 0.000014 | 0.003337 | 0.000007 | 0.120259 | 0.000213 | 305 | 0.283026 | 15.7 | 0.5 | 313 | 335 | 317 | 33 |

| | | | | | | | | | | | | | | |
|---|---|---|---|---|---|---|---|---|---|---|---|---|---|---|
| BS13-10 | 0.283103 | 0.000012 | 0.004073 | 0.000031 | 0.164826 | 0.001725 | 305 | 0.283080 | 17.6 | 0.4 | 229 | 248 | 193 | 28 |
| BS13-12 | 0.282992 | 0.000014 | 0.002776 | 0.000036 | 0.103300 | 0.001440 | 305 | 0.282976 | 13.9 | 0.5 | 387 | 407 | 430 | 31 |
| BS13-18 | 0.283032 | 0.000012 | 0.003451 | 0.000013 | 0.132921 | 0.000557 | 305 | 0.283012 | 15.2 | 0.4 | 333 | 352 | 347 | 28 |
| BS13-19 | 0.282980 | 0.000014 | 0.002663 | 0.000006 | 0.096174 | 0.000219 | 305 | 0.282965 | 13.5 | 0.5 | 403 | 424 | 456 | 32 |
| BS13-22 | 0.282996 | 0.000013 | 0.002952 | 0.000041 | 0.103839 | 0.001426 | 305 | 0.282979 | 14.0 | 0.5 | 383 | 403 | 423 | 31 |
| BS13-23 | 0.283046 | 0.000016 | 0.003174 | 0.000020 | 0.115502 | 0.000748 | 305 | 0.283028 | 15.8 | 0.6 | 309 | 333 | 312 | 36 |
| BS13-24 | 0.283082 | 0.000013 | 0.004146 | 0.000024 | 0.155428 | 0.000917 | 305 | 0.283059 | 16.8 | 0.4 | 262 | 282 | 241 | 29 |
| BS13-25 | 0.283077 | 0.000015 | 0.004699 | 0.000041 | 0.172241 | 0.001606 | 305 | 0.283051 | 16.6 | 0.5 | 274 | 297 | 260 | 33 |
| BS13-26 | 0.283141 | 0.000012 | 0.004962 | 0.000013 | 0.182977 | 0.000396 | 305 | 0.283112 | 18.7 | 0.4 | 175 | 194 | 118 | 27 |
| BS13-27 | 0.283059 | 0.000017 | 0.003747 | 0.000039 | 0.138634 | 0.001430 | 305 | 0.283037 | 16.1 | 0.6 | 295 | 321 | 290 | 39 |
| BS13-28 | 0.282987 | 0.000020 | 0.002587 | 0.000017 | 0.101457 | 0.000695 | 305 | 0.282972 | 13.8 | 0.7 | 392 | 421 | 439 | 45 |
| BS13-30 | 0.282987 | 0.000015 | 0.005096 | 0.000031 | 0.187796 | 0.001287 | 305 | 0.282958 | 13.3 | 0.5 | 422 | 445 | 472 | 33 |

**Table S6.** Whole-rock Sr-Nd isotope data for the Carboniferous igneous rocks from the East Junggar.

| Sample | Age (Ma) | Rb (ppm) | Sr (ppm) | $^{87}Rb/^{86}Sr$ | $^{87}Sr/^{86}Sr$ | 2σ | $(^{87}Sr/^{86}Sr)_i$ | Sm (ppm) | Nd (ppm) | $^{147}Sm/^{144}Nd$ | $^{143}Nd/^{144}Nd$ | 2σ | $\varepsilon_{Nd}(t)$ | $T_{DM1}$ (Ma) | $T_{DM2}$ (Ma) |
|---|---|---|---|---|---|---|---|---|---|---|---|---|---|---|---|
| QK-7 | 340 | 12.5 | 669 | 0.0541 | 0.703940 | 0.000009 | 0.7037 | 6.30 | 32.5 | 0.117052 | 0.512649 | 0.000004 | 3.7 | 791 | 727 |
| QK-8 | 340 | 88.2 | 395 | 0.6462 | 0.706964 | 0.000007 | 0.7038 | 6.82 | 30.2 | 0.136615 | 0.512683 | 0.000003 | 3.5 | 924 | 811 |
| KM-1 | 330 | 64.1 | 605 | 0.3063 | 0.705414 | 0.000007 | 0.7040 | 4.03 | 20.1 | 0.121369 | 0.512767 | 0.000004 | 5.7 | 633 | 622 |
| KM-6 | 330 | 24.5 | 901 | 0.0787 | 0.704312 | 0.000007 | 0.7039 | 5.52 | 23.7 | 0.140863 | 0.512818 | 0.000004 | 5.9 | 695 | 608 |
| BJE-8 | 320 | 13.8 | 489 | 0.0816 | 0.704254 | 0.000008 | 0.7039 | 10.6 | 42.4 | 0.151149 | 0.512889 | 0.000004 | 6.8 | 636 | 527 |
| BJE-9 | 320 | 19.3 | 556 | 0.1004 | 0.704513 | 0.000007 | 0.7041 | 10.6 | 42.2 | 0.151865 | 0.512884 | 0.000004 | 6.6 | 658 | 538 |
| BS-1 | 305 | 68.5 | 506 | 0.3917 | 0.706274 | 0.000004 | 0.7046 | 3.82 | 18.4 | 0.12507927 | 0.512723 | 0.000008 | 4.5 | 735 | 644 |
| BS-13 | 305 | 109 | 70.2 | 4.5040 | 0.726771 | 0.000004 | 0.7072 | 5.11 | 24.4 | 0.12671073 | 0.512846 | 0.000006 | 6.8 | 533 | 482 |

**Table S7.** Whole-rock Pb isotope data for the Carboniferous igneous rocks from the East Junggar.

| Sample | Age (Ma) | Pb (ppm) | Th (ppm) | U (ppm) | $^{206}Pb/^{204}Pb$ | 2σ | $^{207}Pb/^{204}Pb$ | 2σ | $^{208}Pb/^{204}Pb$ | 2σ | $(^{206}Pb/^{204}Pb)_i$ | $(^{207}Pb/^{204}Pb)_i$ | $(^{208}Pb/^{204}Pb)_i$ |
|---|---|---|---|---|---|---|---|---|---|---|---|---|---|
| QK-7 | 340 | 7.16 | 2.80 | 1.25 | 18.5615 | 0.0004 | 15.5494 | 0.0004 | 38.2588 | 0.0013 | 17.962 | 15.517 | 37.824 |
| QK-8 | 340 | 12.2 | 9.88 | 3.10 | 18.8752 | 0.0003 | 15.5800 | 0.0004 | 38.6493 | 0.0012 | 17.996 | 15.533 | 37.744 |
| KM-1 | 330 | 15.6 | 4.88 | 1.59 | 18.3256 | 0.0007 | 15.5383 | 0.0006 | 38.2745 | 0.0018 | 17.987 | 15.520 | 37.937 |
| KM-6 | 330 | 5.80 | 1.83 | 0.89 | 18.2369 | 0.0003 | 15.5171 | 0.0003 | 38.0019 | 0.0009 | 17.728 | 15.490 | 37.664 |
| BJE-8 | 320 | 7.06 | 3.25 | 1.05 | 18.3830 | 0.0009 | 15.5340 | 0.0009 | 38.1798 | 0.0026 | 17.905 | 15.509 | 37.700 |
| BJE-9 | 320 | 7.02 | 3.07 | 1.00 | 18.3894 | 0.0007 | 15.5330 | 0.0007 | 38.1812 | 0.0019 | 17.933 | 15.509 | 37.726 |

**Table S8.** Trace element and isotope data for end-members used in geochemical modelling.

| Geochemical end-members | Sr (ppm) | $(^{87}Sr/^{86}Sr)_i$ | Nd (ppm) | $\varepsilon_{Nd}(t)$ | Pb (ppm) | $(^{206}Pb/^{204}Pb)_i$ |
|---|---|---|---|---|---|---|
| Global Subducting Sediment (GLOSS)[1] | 327 | 0.7173 | 27 | -8.93 | | |
| Upper mantle[2] | 129 | 0.7028 | 12.03 | 8.5 | 0.57 | 18.412 |
| Upper crust[3] | 350 | 0.718 | 26 | -25 | 30 | 19 |
| Lower curst[3] | 300 | 0.71 | 24 | -30 | 4.2 | 15.518 |
| Carboniferous mafic rock (SHJ-32-1)[4] | 1028 | 0.7035 | 26.8 | 7.11 | | |

[1]Data source are from Plank and Langmuir. (1998).

[2]Data source are from Gale et al. (2013).

[3]Data source are from Arslan et al. (2013) and references therein.

[4]Data source are from Zhang et al. (2015).

**Table S9.** Data source for batch melting modelling.

| | Ol | Opx | Cpx | Grt | Sp |
|---|---|---|---|---|---|
| **Mineral and melt modes**[1] | | | | | |
| Garnet lherzolite | 0.6 | 0.2 | 0.1 | 0.1 | |
| Melt (Grt) | 0.03 | -0.16 | 0.88 | 0.09 | |
| spinel lherzolite | 0.53 | 0.27 | 0.17 | | 0.03 |
| Melt (Sp) | -0.06 | 0.28 | 0.67 | | 0.11 |
| **Mineral/liquid distribution coefficients**[2] | | | | | |
| La | 0.0004 | 0.0006 | 0.039 | 0.0014 | 0.0005 |
| Sm | 0.002 | 0.015 | 0.27 | 0.36 | 0.001 |
| Yb | 0.0313 | 0.14 | 0.47 | 6.5 | 0.005 |

[1]Data source of garnet and spinel peridotite sources are from Walter (1998) and Kinzler (1997), respectively.

[2]Data source of mineral/liquid distribution coefficients are from McKenzie and O'Nions (1991), Suhr (1999), Green et al. (2000) and Adam and Green (2006).

**Table S10.** Key geological events in the East Junggar that place constraints on the closure time of the Kalamaili Ocean

| Key events in East Junggar | Location | Sample type | Dating methods/fossil type | age (Ma) | Reference |
|---|---|---|---|---|---|
| Kalamaili ophilites | Kalamaili | Plagiogranite | LA-ICP-MS zircon U-Pb | 417±3 | Huang et al., 2011 |
| | Kalamaili | Gabbro | LA-ICP-MS zircon U-Pb | 407±2; 332±6 | Fang et al., 2015 |
| | Kalamaili | Fossil | Radiolarian | 372-347 | Shu and Wang, 2003 |
| | Kalamaili | Plagiogranite | SIMS zircon U-Pb (SHRIMP) | 373±10 | Tang et al., 2007a |
| | Kalamaili | Quartz diorite | LA-ICP-MS zircon U-Pb | 371±3 | Liu et al., 2017 |
| | Zhifang | MORB-type layered rocks | SIMS zircon U-Pb (CAMECA) | 377±1 | Xu et al., 2015 |
| | Alekuntunduo | Plagiogranite | SIMS zircon U-Pb (SHRIMP) | 351±6 | Qin, 2012 |
| | Kalamaili | MORB-type Gabbro | LA-ICP-MS zircon U-Pb | 330±2 | Wang et al., 2009 |
| Fossils | Kalamaili | Radiolarian | *Palaeoscenidium cladophorum* Deflandre, *Entactinosphaera palimbola* Foreman, *Trianosphaera sicarius* Deflandre | 372-347 | Shu and Wang, 2003 |
| | Kalamaili | Angara flora | *Angaropteridium cf. Cordiopteroides(Schmain.,Zai), Noggerothiopsis* sp.,*N.cf.Theodori Tschirkovaet Zalossky, N.subangusta Zalessky, Calamites* sp. | 318-290 | Zhu et al., 2005; Zhang et al., 2009 |
| A-type granites | Northern subarea | Alkaline granite | LA-ICP-MS zircon U-Pb | 325±2; 322±2 | Liu et al., 2013 |
| | Ulungur pluton | Alkaline granite | LA-ICP-MS zircon U-Pb | 323±4; 320±5; 319±4; 319±3 | Tang et al., 2020 |
| | Wucaicheng pluton | Alkaline granite | LA-ICP-MS zircon U-Pb | 321±2 | Tian et al., 2016 |
| | Sabei pluton | Alkaline granite | SIMS zircon U-Pb (SHRIMP) | 314±5; 313±2 | Lin et al., 2007 |
| | Huangyanshan pluton | Alkaline granite | LA-ICP-MS zircon U-Pb | 311±5 | Yang et al., 2011 |
| | Southern subarea | Alkaline granite | LA-ICP-MS zircon U-Pb | 311±2; 304±2; 301±2 | Liu et al., 2013 |
| | Huangyanshan pluton | Alkaline granite | LA-ICP-MS zircon U-Pb | 310±4; 302±2 | Su et al., 2007 |
| | Ulungur pluton | Alkaline granite | Whole-rock Rb-Sr dating | 308±14; 304±32; 303±26; 300±6 | Han et al., 1997 |
| | Sabei pluton | Alkaline granite | LA-ICP-MS zircon U-Pb | 306±3 | Su et al., 2007 |
| | Sabei pluton | Alkaline granite | LA-ICP-MS zircon U-Pb | 306±3 | Tang et al., 2007b |
| | Huangyanshan pluton | Alkaline granite | Whole-rock and mineral Rb-Sr dating | 294±1; 281±6; 278±6 | Chen and Jahn, 2004 |

| | | | | | |
|---|---|---|---|---|---|
| | Daliugou pluton | Bi monzogranite | SIMS zircon U-Pb (SHRIMP) | 288±3 | Yuan et al., 2010 |
| | Dajiashan pluton | Alkaline granite | SIMS zircon U-Pb (SHRIMP) | 287±2 | Yuan et al., 2010 |
| | Barkol Tagh pluton | Bi monzogranite | SIMS zircon U-Pb (SHRIMP) | 284±5 | Yuan et al., 2010 |
| | Beilekuduke pluton | Bi-Kf granite | LA-ICP-MS zircon U-Pb | 283±2 | Yang et al., 2011 |
| Stitching intrusions | Wucaicheng | Hornblende gabbro | LA-ICP-MS zircon U-Pb | 319±3 | Tian et al., 2016 |
| | Sikeshu pluton | Granodiorite | SIMS zircon U-Pb (SHRIMP) | 316±3 | Han et al., 2010 |
| Molasse deposits | Shuangjingzi | Molasse | SIMS zircon U-Pb (SHRIMP) | 345-343.5 | Zhang et al., 2013 |
| Early Carboniferous Island-arc magmatism | Shuangjingzi | Mafic-intermedicate voclanic rocks | LA-ICP-MS zircon U-Pb | 353±3; 351±3; 335±3; 331±2 | Li et al., 2020 |
| | Qiakuerite | Mafic-intermedicate voclanic rocks | LA-ICP-MS zircon U-Pb | 340±8; 341±4 | This study |
| | Northern Kalamaili fault | Mafic voclanic rocks | Based on the strata | 340 | Zhang et al., 2009 |
| | Baijiangou | Keratophyre; Rhyolite | LA-ICP-MS zircon U-Pb | 336±2; 332±9 | Xiao et al., 2011 |
| | Huofu and Hongjianshan | Mafic voclanic rocks | Based on the strata | 335 | Su et al., 2012 |
| | Kamste | Mafic-intermedicate voclanic rocks | LA-ICP-MS zircon U-Pb | 334±4; 328±4 | This study |
| | Eastern Junggar Basin | Bimodal volcanic rocks | LA-ICP-MS zircon U-Pb | 334-336 | Wang et al., 2021 |
| Late Carboniferous post-collisional magmatism | Baijiandong | Mafic dikes | Whole-rock $^{40}Ar$-$^{39}Ar$ dating | 320±2 | This study |
| | Zhaheba | Mafic-intermedicate voclanic rocks | LA-ICP-MS zircon U-Pb | 317±2; 315±2 | Li et al., 2014 |
| | Northern Kalamaili fault | Mafic voclanic rocks | Based on the strata | 310 | Zhang et al., 2009 |
| | BS | Felsic volcanic rocks | LA-ICP-MS zircon U-Pb | 305±2 | This study |
| | Shiquanzi | Mafic-intermedicate voclanic rocks | LA-ICP-MS zircon U-Pb | 301±6 | Yuan et al., 2010 |
| | Eastern Junggar Basin | Basalt | LA-ICP-MS zircon U-Pb | 300±1 | Su et al., 2010 |
| | Kalamaili | Bimodal volcanic rocks | LA-ICP-MS zircon U-Pb | 320±4 | Luo et al., 2017 |
| | Baijiandong | Bimodal volcanic rocks | LA-ICP-MS zircon U-Pb | 314±2; 307±2 | Su et al., 2012 |

## REFERENCES CITED


Adam, J., and Green, T., 2006, Trace element partitioning between mica- and amphibole-bearing garnet lherzolite and hydrous basaltic melt: 1. Experimental results and the investigation of controls on partitioning behaviour: Contributions to Mineralogy and Petrology, v. 152, p. 1–17, https://doi.org/10.1007/s00410-006-0085-4.

Arslan, M., Temizel, İ., Abdioğlu, E., Kolaylı, H., Yücel, C., Boztuğ, D., and Şen, C., 2013, $^{40}Ar$-$^{39}Ar$ dating, whole-rock and Sr-Nd-Pb isotope geochemistry of post-collisional Eocene volcanic rocks in the southern part of the Eastern Pontides (NE Turkey): implications for magma evolution in extension-induced origin: Contributions to Mineralogy and Petrology, v. 166, p. 113–142, https://doi.org/10.1007/s00410-013-0868-3.

Baker, J., Peate, D., Waight, T., and Meyzen, C., 2004, Pb isotopic analysis of standards and samples using a $^{207}Pb$-$^{204}Pb$ double spike and thallium to correct for mass bias with a double-focusing MC-ICP-MS: Chemical Geology, v. 211, p. 275–303, https://doi.org/10.1016/j.chemgeo.2004.06.030.

Chen, B., and Jahn, B.M., 2004, Genesis of post-collisional granitoids and basement nature of the Junggar Terrane, NW China: Nd-Sr isotope and trace element evidence: Journal of Asian Earth Sciences, v. 23, p. 691–703, https://doi.org/10.1016/S1367-9120(03)00118-4.

Fang, A.M., Wang, S.G., Zhang, J.M., Zang, M., Fang, J.H., and Hu, J.M., 2015, The U-Pb ages of zircons from the gabbro in the Kalamaili ophiolite, North Xinjiang and its tectonic significances [in Chinese with English abstract]: Chinese Journal of Geology, v. 50, p. 140–154.

Gale, A., Dalton, C.A., Langmuir, C.H., Su, Y., and Schilling, J.G., 2013, The mean composition of ocean ridge basalts: Geochemistry Geophysics Geosystems, v. 14, p. 489–518, https://doi.org/10.1029/2012GC004334.

Green, T.H., Blundy, J.D., Adam, J., and Yaxley, G.M., 2000, SIMS determination of trace element partition coefficients between garnet, clinopyroxene and hydrous basaltic liquids at 2–7.5 GPa and 1080–1200 °C: Lithos, v. 53, p. 165–187, https://doi.org/10.1016/S0024-4937(00)00023-2.

Griffin, W.L., Pearson, N.J., Belousova, E.A., Jackson, S.E., Van Achterbergh, E., O'Reilly, S.Y., and Shee, S.R., 2000, The Hf isotope composition of cratonic mantle: LAM-MC-ICPMS analysis of zircon megacrysts in kimberlites: Geochimica et Cosmochimica Acta, v. 64, p. 133–147, https://doi.org/10.1016/S0016-7037(99)00343-9.

Han, B.F., Wang, S.G., Jahn, B.M., Hong, D.W., Kagami, H., and Sun, Y.L., 1997, Depleted-mantle source for the Ulungur River A-type granites from North Xinjiang, China: geochemistry and Nd-Sr isotopic evidence, and implications for Phanerozoic crustal growth: Chemical Geology, v. 138, p. 135–159, https://doi.org/10.1016/S0009-2541(97)00003-X.

Han, B.F., Guo, Z.J., Zhang, Z.C., Zhang, L., Chen, J.F., and Song, B., 2010, Age, geochemistry, and tectonic implications of a late Paleozoic stitching pluton in the North Tian Shan suture zone, western China: Geological Society of America Bulletin, v. 122, p. 627–640, https://doi.org/10.1130/B26491.1.

Hu, Z.C., Liu, Y.S., Gao, S., Liu, W., Yang, L., Zhang, W., Tong, X., Lin, L., Zong, K.Q., Li, M., Chen, H., and Zhou, L., 2012, Improved in situ Hf isotope ratio analysis of zircon using newly designed X skimmer cone and Jet sample cone in combination with the addition of nitrogen by laser ablation multiple collector ICP-MS: Journal of Analytical Atomic Spectrometry, v. 27, p. 1391–1399, https://doi.org/10.1039/c2ja30078h.

Hu, Z.C., Zhang, W., Liu, Y.S., Gao, S., Li, M., Zong, K.Q., Chen, H.H., and Hu, S.H., 2015, "Wave" signal-smoothing and mercury-removing device for laser ablation quadrupole and multiple collector ICPMS analysis: application to lead isotope analysis: Analytical Chemistry, v. 87, p. 1152–1157, https://doi.org/10.1021/ac503749k.
Huang, G., Zhang, Z.W., Dong, Z.H., and Zhang, W.F., 2011, Zircon LA-ICP-MS U-Pb age of plagiogranite from Tonghuashan ophiolite in Southern Tianshan Mountains and its geological implications: Geology in China, v. 38, p. 102–107.
Kinzler, R.J., 1997, Melting of mantle peridotite at pressure approaching the spinel to garnet transition: Application to mid-ocean ridge basalt petrogenesis: Journal of Geophysical Research, v. 102, p. 853–874, https://doi.org/10.1029/96JB00988.
Koppers, A.A.P., 2002, ArArCALC-software for $^{40}Ar/^{39}Ar$ age calculations: Computers & Geosciences, v. 28, p. 605–619, https://doi.org/10.1016/S0098-3004(01)00095-4.
Li, C.F., Li, X.H., Li, Q.L., Guo, J.H., and Yang, Y.H., 2012, Rapid and precise determination of Sr and Nd isotopic ratios in geological samples from the same filament loading by thermal ionization mass spectrometry employing a single-step separation scheme: Analytica Chimica Acta, v. 727, p. 54–60, https://doi.org/10.1016/j.aca.2012.03.040.
Li, D., He, D.F., Santosh, M., and Tang, J.Y., 2014, Petrogenesis of Late Paleozoic volcanics from the Zhaheba depression, East Junggar: Insights into collisional event in an accretionary orogen of Central Asia: Lithos, v. 184–187, p. 167–193, https://doi.org/10.1016/j.lithos.2013.10.003.
Li, D., He, D.F., Sun, M., and Zhang, L., 2020, The role of Arc-Arc Collision in Accretionary Orogenesis: Insights From ~320 Ma Tectono-sedimentary Transition in the Karamaili Area, NW China: Tectonics, v. 39, e2019TC005623.
Lin, J.F., Yu, H.X., Yu, X.Q., Di, Y.J., and Tian, J.T., 2007, Zircon SHRIMP U-Pb dating and geological implication of the Sabei alkali-rich granite from Eastern Junggar of Xinjiang, NW China [in Chinese with English abstract]: Yanshi Xuebao, v. 23, p. 1876–1884.
Liu, W., Liu, X.J., and Liu, L.J., 2013, Underplating generated A- and I-type granitoids of the East Junggar from the lower and the upper oceanic crust with mixing of mafic magma: Insights from integrated zircon U-Pb ages, petrography, geochemistry and Nd-Sr-Hf isotopes: Lithos, v. 179, p. 293–319, https://doi.org/10.1016/j.lithos.2013.08.009.
Liu, X.J., Xiao, W.J., Xu, J.F., Castillo, P.R., and Shi, Y., 2017, Geochemical signature and rock associations of ocean ridge-subduction: Evidence from the Karamaili Paleo-Asian ophiolite in east Junggar, NW China: Gondwana Research, v. 48, p. 34–49, https://doi.org/10.1016/j.gr.2017.03.010.
Liu, Y.S., Hu, Z.C., Gao, S., Günther, D., Xu, J., Gao, C.G., and Chen, H.H., 2008, In situ analysis of major and trace elements of anhydrous minerals by LA-ICP-MS without applying an internal standard: Chemical Geology, v. 257, p. 34–43, https://doi.org/10.1016/j.chemgeo.2008.08.004.
Liu, Y.S., Gao, S., Hu, Z.C., Gao, C.G., Zong, K.Q., and Wang, D.B., 2010, Continental and oceanic crust recycling-induced melt-peridotite interactions in the Trans-North China Orogen: U-Pb dating, Hf isotopes and trace elements in zircons from mantle xenoliths: Journal of Petrology, v. 51, p. 537–571, https://doi.org/10.1093/petrology/egp082.
Ludwig, K.R., 2003, Isoplot/Ex, Version 3: A Geochronological Toolkit for Microsoft Excel: Berkeley Geochronology Center Special Publication 4, 70 p.
Luo, T., Liao, Q., Chen, J., Hu, C., Wang, F., Chen, S., Wu, W., Tian, J., and Fan, G., 2017, A record of post-collisional transition: evidence from geochronology and geochemistry of

Paleozoic volcanic rocks in the eastern Junggar, Central Asia: International Geology Review, v. 59, p. 1256–1275, https://doi.org/10.1080/00206814.2016.1160800.
Ma, Q., Zheng, J.P., Griffin, W.L., Zhang, M., Tang, H.Y., Su, Y.P., and Ping, X.Q., 2012, Triassic "adakitic" rocks in an extensional setting (North China): melts from the cratonic lower crust: Lithos, v. 149, p. 159–173, https://doi.org/10.1016/j.lithos.2012.04.017.
McKenzie, D.P., and O'Nions, R.K., 1991, Partial melt distributions from inversion of rare earth element concentrations: Journal of Petrology, v. 32, p. 1021–1091, https://doi.org/10.1093/petrology/32.5.1021.
Qin, B., 2012, Time constraints and SHRIMP of zircon from plagioclase granite of ophiolitic in Aletunkunduo [in Chinese with English abstract]: Northwest Geology, v. 45, p. 20–25.
Qiu, H.N., Bai, X.J., and Liu, W.G., 2015, Automatic $^{40}Ar/^{39}Ar$ dating technique using multicollector ArgusVI MS with home-made apparatus [in Chinese with English abstract]: Geochimica, v. 44, p. 477–484.
Shu, L.S., and Wang, Y.J., 2003, Late Devonian–early Carboniferous radiolarian fossils from siliceous rocks of the Kalamaili ophiolite, Xinjiang: Dizhi Lunping, v. 4, p. 408–412.
Su, Y.P., Tang, H.F., Sylvester, P.J., Liu, C.Q., Qu, W.J., Hou, G.S., and Cong, F., 2007, Petrogenesis of Karamaili alkaline A-type granites from East Junggar, Xinjiang (NW China) and their relationship with tin mineralization: Geochemical Journal, v. 41, p. 341–357, https://doi.org/10.2343/geochemj.41.341.
Su, Y.P., Zheng, J.P., Griffin, W.L., Tang, H.Y., O'Reilly, S.Y., and Lin, X.Y., 2010, Zircon U-Pb and Hf isotopes of volcanic rocks from the Batamayineishan Formation in the eastern Junggar Basin: Chinese Science Bulletin, v. 55, p. 4150–4161, https://doi.org/10.1007/s11434-010-4151-y.
Su, Y.P., Zheng, J.P., Griffin, W.L., Zhao, J.H., Tang, H.Y., Ma, Q., and Lin, X.Y., 2012, Geochemistry and geochronology of Carboniferous volcanic rocks in the eastern Junggar terrane, NW China: implication for a tectonic transition: Gondwana Research, v. 22, p. 1009–1029, https://doi.org/10.1016/j.gr.2012.01.004.
Suhr, G., 1999, Melt Migration under Oceanic Ridges: Inferences from Reactive Transport Modelling of Upper Mantle Hosted Dunites: Journal of Petrology, v. 40, p. 575–599, https://doi.org/10.1093/petroj/40.4.575.
Tang, G.J., Wang. Q., Wyman, D.A., Dan. W., Ma. L., Zhang. H.X., and Zhao. Z.H., 2020, Petrogenesis of the Ulungur Intrusive Complex, NW China, and Implications for Crustal Generation and Reworking in Accretionary Orogens: Journal of Petrology, v. 61, egaa018.
Tang, H.F., Su, Y.P., Liu, C.Q., Hou, G.S., and Wang, Y.B., 2007a, Zircon U-Pb age of the plagiogranite in Kalamaili Belt, northern Xinjiang and its tectonic implications [in Chinese with English abstract]: Geotectonica et Metallogenia, v. 31, p. 110–117.
Tang, H.F., Qu, W.J., Su, Y.P., Hou, G.S., Du, A.D., and Cong, F., 2007b, Genetic connection of Sareshike tin deposit with the alkaline A-type granites of Sabei body in Xinjiang: constraint from isotopic ages [in Chinese with English abstract]: Yanshi Xuebao, v. 23, p. 1989–1997.
Tian, J., Liao, Q.A., Fan, G.M., Nie, X.M., Hu, C.B., Wang, F.M., Chen, S., and Wu, W.W., 2016, Mantle underplated pluton and stitching granite pluton from south side of the Karamaili fault in eastern Junggar: geochronological, geochemical and Sr-Nd isotopic constraints on their petrogenesis and tectonic implications [in Chinese with English abstract]: Yanshi Xuebao, v. 32, p. 1715–1730.

Wang, B.Y., Jiang, C.Y., Li, Y.J., Wu, H.E., Xia, Z.D., and Lu, R.H., 2009, Geochemistry and tectonic implications of Karamaili ophiolite in East Junggar of Xinjiang [in Chinese with English abstract]: Journal of Mineralogy and Petrology, v. 29, p. 74–82.
Wang, J., Su, Y.P., Zheng, J.P., Belousova, E.A., Chen, M., Dai, H., and Zhou, X., 2021, Petrogenesis of early Carboniferous bimodal-type volcanic rocks from the Junggar Basin (NW China) with implications for Phanerozoic crustal growth in Central Asian Orogenic Belt: Gondwana Research, v. 89, p. 220–237, https://doi.org/10.1016/j.gr.2020.10.008.
Walter, M.J., 1998, Melting of garnet peridotite and the origin of komatiite and depleted lithosphere: Journal of Petrology, v. 39, p. 29–60, https://doi.org/10.1093/petroj/39.1.29.
Xiao, Y., Zhang, H.F., Shi, J.A., Su, B.X., Sakyi, P.A., Lu, X.C., Hu, Y., and Zhang, Z., 2011, Late Paleozoic magmatic record of East Junggar, NW China and its significance: Implication from zircon U-Pb dating and Hf isotope: Gondwana Research, v. 20, p. 532–542, https://doi.org/10.1016/j.gr.2010.12.008.
Xu, X.W., Jiang, N., Li, X.H., Wu, C., Qu, X., Zhou, G., and Dong, L.H., 2015, Spatial-temporal framework for the closure of the Junggar Ocean in central Asia: New SIMS zircon U-Pb ages of the ophiolitic mélange and collisional igneous rocks in the Zhifang area, East Junggar: Journal of Asian Earth Sciences, v. 111, p. 470–491, https://doi.org/10.1016/j.jseaes.2015.06.017.
Yang, G.X., Li, Y.J., Wu, H.G., Zhong, X., Yang, B.K., Yan, C.X., Yan, J., and Si, G.H., 2011, Geochronological and geochemical constrains on petrogenesis of the Huangyangshan A-type granite from the East Junggar, Xinjiang, NW China: Journal of Asian Earth Sciences, v. 40, p. 722–736, https://doi.org/10.1016/j.jseaes.2010.11.008.
Yuan, C., Sun, M., Wilde, S., Xiao, W.J., Xu, Y.G., Long, X.P., and Zhao, G.C., 2010, Post-collisional plutons in the Balikun area, East Chinese Tianshan: Evolving magmatism in response to extension and slab break-off: Lithos, v. 119, p. 269–288, https://doi.org/10.1016/j.lithos.2010.07.004.
Zhang, Y.Y., Pe-Piper, G., Piper, D.J.W., and Guo, Z.J., 2013, Early Carboniferous collision of the Kalamaili orogenic belt, North Xinjiang, and its implications: evidence from molasse deposits: Geological Society of America Bulletin, v. 125, p. 932–944, https://doi.org/10.1130/B30779.1.
Zhang, Y.Y., Guo, Z.J., Pe-Piper, G., and Piper, D.J.W., 2015, Geochemistry and petrogenesis of Early Carboniferous volcanic rocks in East Junggar, North Xinjiang: Implications for post-collisional magmatism and geodynamic process: Gondwana Research, v. 28, p. 1466–1481, https://doi.org/10.1016/j.gr.2014.08.018.
Zhang, Z.C., Zhou, G., Kusky, T.M., Yan, S.H., Chen, B.L., and Zhao, L., 2009, Late Paleozoic volcanic record of the Eastern Junggar terrane, Xinjiang, Northwestern China: Major and trace element characteristics, Sr-Nd isotopic systematics and implications for tectonic evolution: Gondwana Research, v. 16, p. 201–215, https://doi.org/10.1016/j.gr.2009.03.004.
Zhu, Z.X., Li, S.Z., and Li, G.L., 2005, The characteristics of sedimentary system–continental facies volcano in later Carboniferous Batamayi group, Zhifang region [in Chinese with English abstract]: East Junggar: Xinjiang Geology, v. 23, p. 14–18.
Zong, K.Q., Klemd, R., Yuan, Y., He, Z.Y., Guo, J.L., Shi, X.L., Liu, Y.S., Hu, Z.C., and Zhang, Z.M., 2017, The assembly of Rodinia: the correlation of early Neoproterozoic (ca. 900 Ma) high-grade metamorphism and continental arc formation in the southern Beishan Orogen, southern Central Asian Orogenic Belt (CAOB): Precambrian Research, v. 290, p. 32–48, https://doi.org/10.1016/j.precamres.2016.12.010.

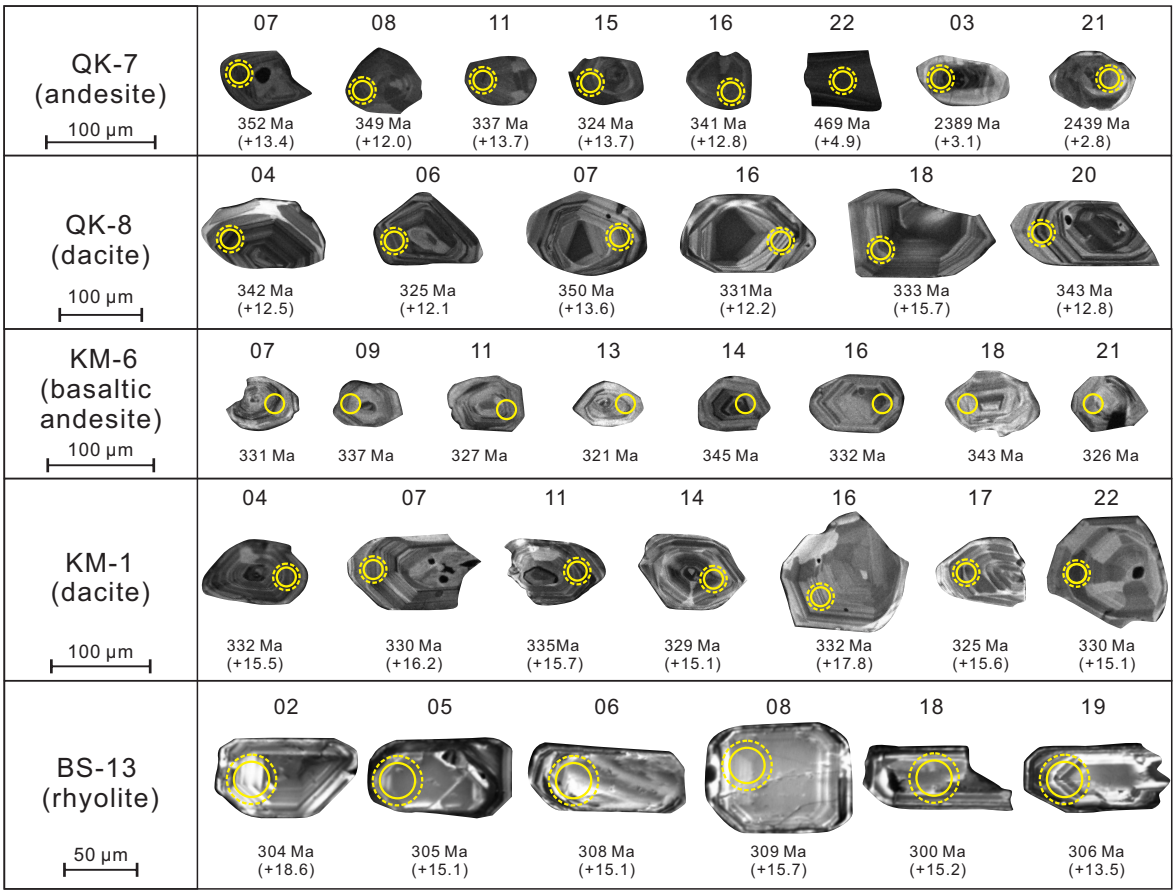
QK-7
(andesite)
100 μm
07
352 Ma
(+13.4)
08
349 Ma
(+12.0)
11
337 Ma
(+13.7)
15
324 Ma
(+13.7)
16
341 Ma
(+12.8)
22
469 Ma
(+4.9)
03
2389 Ma
(+3.1)
21
2439 Ma
(+2.8)
QK-8
(dacite)
100 μm
04
342 Ma
(+12.5)
06
325 Ma
(+12.1
07
350 Ma
(+13.6)
16
331Ma
(+12.2)
18
333 Ma
(+15.7)
20
343 Ma
(+12.8)
KM-6
(basaltic
andesite)
100 μm
07
331 Ma
09
337 Ma
11
327 Ma
13
321 Ma
14
345 Ma
16
332 Ma
18
343 Ma
21
326 Ma
KM-1
(dacite)
100 μm
04
332 Ma
(+15.5)
07
330 Ma
(+16.2)
11
335Ma
(+15.7)
14
329 Ma
(+15.1)
16
332 Ma
(+17.8)
17
325 Ma
(+15.6)
22
330 Ma
(+15.1)
BS-13
(rhyolite)
50 μm
02
304 Ma
(+18.6)
05
305 Ma
(+15.1)
06
308 Ma
(+15.1)
08
309 Ma
(+15.7)
18
300 Ma
(+15.2)
19
306 Ma
(+13.5)

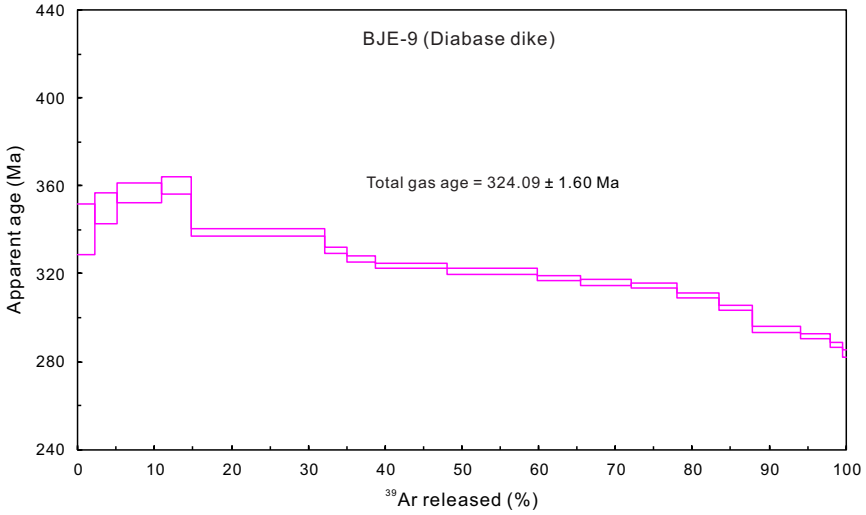
BJE-9 (Diabase dike)
Total gas age = 324.09 ± 1.60 Ma
Apparent age (Ma)
440
400
360
320
280
240
0
10
20
30
40
50
60
70
80
90
100
39Ar released (%)